Journal of Aerosol Science 168 (2023) 106102

Contents lists available at ScienceDirect

Journal of Aerosol Science

journal homepage: www.elsevier.com/locate/jaerosci

Size, concentration, and origin of human exhaled particles and their dependence on human factors with implications on infection transmission

Gholamhossein Bagheri [a,*], Oliver Schlenczek [a], Laura Turco [a], Birte Thiede [a], Katja Stieger [a,b], Jana M. Kosub [c], Sigrid Clauberg [c], Mira L. Pöhlker [d,e], Christopher Pöhlker [d], Jan Moláček [a], Simone Scheithauer [c], Eberhard Bodenschatz [a,b,f,*]

[a] Max Planck Institute for Dynamics and Self-Organization (MPIDS), Göttingen 37077, Germany
[b] Institute for Dynamics of Complex Systems, University of Göttingen, Göttingen 37077, Germany
[c] Department of Infection Control and Infectious Diseases, University Medical Center and University of Göttingen 37075, Germany
[d] Multiphase Chemistry Department, Max Planck Institute for Chemistry, Mainz 55128, Germany
[e] Experimental Aerosol and Cloud Microphysics Department, Leibniz Institute for Tropospheric Research, 04318 Leipzig, Germany
[f] Laboratory of Atomic and Solid State Physics and Sibley School of Mechanical and Aerospace Engineering, Cornell University, Ithaca, NY 14853, USA

ARTICLE INFO

Editor: Dr. Chris Hogan

Dataset link: https://aerosol.ds.mpg.de/en/

Keywords:
Respiratory particle
Aerosol
Droplet
Transmission risk
Airborne
Infection prevention

ABSTRACT

Understanding infection transmission between individuals, as well as evaluating the efficacy of protective measures, are key issues in pandemics driven by human respiratory particles. The key is a quantitative understanding of the size and concentration of particles exhaled and their variability across the size range for a representative population of all ages, genders, and different activities. Here we present data from 132 healthy volunteers aged 5 to 80 years, measured over the entire particle size range for each individual. Conventional particle spectrometry was combined with in-line holography under well-controlled conditions for common activities such as breathing, speaking, singing, and shouting. We find age to be the most important parameter for the concentration of small exhale particles <5 μm (PM5), which doubles over a 7-year period in adolescents and over a 30-year period in adults. Gender, body mass index, smoking or exercise habits have no discernible effect. We provide evidence that particles with a diameter of <5 μm originate from the lower respiratory tract, 5–15 μm from the larynx/pharynx, and >15 μm from the oral cavity. PM5 concentration can vary by one order of magnitude within a person, while inter-person variability can span two orders of magnitude, largely explained by difference in age. We found no discernible inter-person variability for particles larger than 5 μm. Our results show that cumulative volume of PM5 is 2–8 times higher in adults than in children. In contrast, number and volume concentration of larger particles, which are produced predominantly in the upper respiratory tract, is largely independent of age. Finally, we examined different types of airborne-transmissible respiratory diseases and provided insights into possible modes of infection transmission with and without several types/fits of face masks.

* Corresponding authors.
E-mail addresses: gholamhossein.bagheri@ds.mpg.de (G. Bagheri), eberhard.bodenschatz@ds.mpg.de (E. Bodenschatz).

https://doi.org/10.1016/j.jaerosci.2022.106102
Received 1 August 2022; Received in revised form 14 October 2022; Accepted 12 November 2022
Available online 21 November 2022

1. Introduction

Human exhalations contain endogenously generated particles, composed of non-volatile substances, such as salts, proteins, water and, if they are infectious, pathogens. These particles span in size from nanometers to millimeters and are referred to as aerosols and/or droplets (Alsved, et al., 2020; Asadi, et al., 2019; Bake, Larsson, Ljungkvist, Ljungström, & Olin, 2019; Chao, et al., 2009; Duguid, 1946; Holmgren, Bake, Olin, & Ljungström, 2011; Johnson & Morawska, 2009; Loudon & Roberts, 1967; Merghani, Sagot, Gehin, Da, & Motzkus, 2021; Morawska, et al., 2009a; Pöhlker, et al., 2021; Randall, Ewing, Marr, Jimenez, & Bourouiba, 2021; Xie, Li, Sun, & Liu, 2009). Knowledge of situation-dependent particle number concentrations exhaled by an infectious individual is central for understanding contact-free-transmitted diseases. This applies to the current COVID-19 pandemic as well as to other infectious diseases of viral or bacterial origin, e.g. chickenpox, influenza, measles and tuberculosis.

The concrete knowledge of all transmission routes, which are classically divided into contact-free (airborne, droplet) and contact transmission (Siegel, Rhinehart, Jackson, & Chiarello, 2007), is the basic prerequisite for the development and implementation of the appropriate infection control and hygiene measures. Furthermore, it is necessary to distinguish between the risk for near-field transmission in the vicinity of an infectious and far-field transmission for example by the infectious "air" in a room. Transmission can occur anywhere indoors as well as outdoors yet with vastly different transmission probabilities. Limiting contact-free-transmission requires disproportionately intensive and costly hospital and public health interventions. The range of measures to disrupt disease transmission in general has been well researched in the past. However, during the SARS-CoV-2 pandemic, it became clear that our knowledge of human exhaled aerosols and droplets is insufficient in terms of the concentrations expected to be released into the air during various activities such as breathing, talking and shouting. In particular a knowledge of the inter human variability is paramount to predict the variability in transmission risk and little to no data can be found in the literature.

The most important variable for assessing the risk of disease transmission by human exhaled particles is the source, which is given by the size and concentration of particles exhaled by the infectious individual. There are a significant number of studies in the literature dealing with exactly this topic (Almstrand, et al., 2009; Alsved, et al., 2020; Asadi, et al., 2019; Chao, et al., 2009; Duguid, 1946; Fabian, Brain, Houseman, Gern, & Milton, 2011; Fabian, et al., 2008; Gregson, et al., 2021; Han, Weng, & Huang, 2013; Haslbeck, Schwarz, Hohlfeld, Seume, & Koch, 2010; Holmgren et al., 2011; Holmgren, et al., 2013; Holmgren, Ljungström, Almstrand, Bake, & Olin, 2010; Johnson & Morawska, 2009; Johnson, et al., 2011; Lai, Bottomley, & McNerney, 2011; Lee, et al., 2019; Li, Niu, & Zhu, 2020; Loudon & Roberts, 1967; Morawska, et al., 2008, 2009a; Mürbe, et al., 2021; Papineni & Rosenthal, 1997; Schwarz, Biller, Windt, Koch, & Hohlfeld, 2010, 2015; Smith, et al., 2020; Xie et al., 2009). These studies have provided valuable information on the size and concentration of particles generated by different breathing maneuvers, and have provided insights into the mechanisms of particle generation and possible airborne transmission routes. Nevertheless, important details remain unresolved. Some studies have focused on a narrow particle size range (Almstrand, et al., 2010, 2009; Alsved, et al., 2020; Asadi, et al., 2019; Fabian, et al., 2011, 2008; Gregson, et al., 2021; Haslbeck, et al., 2010; Holmgren et al., 2011; Holmgren, et al., 2013, 2010; Johnson & Morawska, 2009; Lai et al., 2011; Li et al., 2020; Morawska, et al., 2008, 2009b; Mürbe, et al., 2021; Papineni & Rosenthal, 1997; Schwarz, et al., 2010, 2015), or did not perform direct concentration measurements (Chao, et al., 2009; Duguid, 1946; Loudon & Roberts, 1967; Xie et al., 2009), or did not perform measurements in a cleanroom and/or with control of the relative humidity of the samples (Asadi, et al., 2019; Duguid, 1946; Fabian, et al., 2011, 2008; Han et al., 2013; Loudon & Roberts, 1967), or provided data with comparatively low size resolution (Fabian, et al., 2011, 2008; Lai et al., 2011; Lee, et al., 2019; Schwarz, et al., 2010, 2015), or did not provide sufficient information to reliably determine particle size distributions (Han et al., 2013; Papineni & Rosenthal, 1997; Smith, et al., 2020), or involved very few subjects (less than 10) in their study (Almstrand, et al., 2009; Duguid, 1946; Holmgren et al., 2011; Lai et al., 2011; Li et al., 2020; Loudon & Roberts, 1967; Mürbe, et al., 2021; Papineni & Rosenthal, 1997; Smith, et al., 2020; Xie et al., 2009) or did not investigate activities associated with vocalization (Almstrand, et al., 2009, 2009; Fabian, et al., 2011, 2008; Haslbeck, et al., 2010, 2010; Holmgren et al., 2011; Holmgren, et al., 2013, 2010; Johnson & Morawska, 2009; Schwarz, et al., 2010, 2015). Moreover, there are almost no data for children and adolescents (Mürbe, et al., 2021; Pöhlker, et al., 2021). This is all the more important because (i) children and young adults spend more time indoors (e.g. schools, daycare, kindergarden), (ii) may show fewer symptoms even though they are fully infectious, and (iii) may be handicapped in their development by strict infection prevention methods such as social distancing. Finally, to our knowledge, no study to date has directly measured the concentration of particles $>20\,\mu m$.

It is precisely the knowledge of what is not known that is the key to a more quantitative determination of transmission routes. For this, precise knowledge of the concentration, size and shrinkage of exhaled particles in all age groups is essential. In addition, possible differences due to age, gender or factors such as BMI, smoking and exercise may be of particular importance. If no differences are found in relation to an influencing factor, the measures can be developed independently of this factor. However, if there is a dependence, e.g., on age, this would not only explain differences in transmission probabilities, but also provide the basis for situation-specific interventions, thus providing more effective and appropriate interventions to minimize transmission.

Here we fill this knowledge gap by carrying out extensive measurements on exhalations of 132 subjects in age range of 5–80 years using Particle Size Spectrometers (PSSs) and in-line holography in a better than ISO Class 4 cleanroom. Subjects performed nose/mouth breathing, normal/loud speaking, singing, humming, shouting and other specific activities (e.g. singing/shouting with open mouth). Respiratory particles larger than $6\,\mu m$ were directly measured with in-line holography, a proven instrument in the field of atmospheric cloud microphysics (Schlenczek, 2018), just a few centimeters from the mouth and nose of the subject; particles $<10\,\mu m$ were measured using the PSSs after exhalation was captured via specifically designed full-face masks and also by sampling with a funnel in front of the subjects mouth/nose for the same activities. The dependencies of the data on gender, age, vocal sound pressure, height and body mass index (BMI) are discussed in detail. Furthermore, discussions of the significance of the provided data and implications for placing infection control measures, in particular face masks, for different types of contact-free infectious agents from the human respiratory tract is also presented.

Table 1
Overview of subjects and samples analyzed per activities and instrument. Number of samples for measurements carried out with PSSs is the total duration of measurements in minutes while for the those carried out with in-line holography is the total number of holograms with particles in the central region (i.e., the effective sampling volume).

Activity	No. Subj.	Age Min-Max (Med.)	No. Samp.	No. Exps. (female%)
SMPS (and APS)				
Breathing	40	21–64 (35)	218	47 (36)
Norm. speak	41	21–64 (35)	285	87 (40)
Loud. speak	41	21–64 (35)	281	87 (39)
Singing	41	21–64 (35)	247	89 (44)
Shouting	6	31–64 (38)	10	10 (20)
OPS				
Breathing	131	5–80 (27)	1050	234 (37)
Norm. speak	129	5–80 (22)	1005	251 (42)
Loud. speak	132	5–80 (24)	1035	257 (41)
Singing	132	5–80 (28)	809	281 (40)
Humming	60	5–70 (14)	207	66 (42)
Shouting	40	5–61 (31)	56	56 (28)
Holography				
Norm. speak	88	5–80 (28)	897	91 (37)
Loud. speak	91	5–74 (30)	2162	98 (40)
Singing	81	5–74 (35)	1700	95 (40)
Shouting	4	35–61 (36)	309	9 (0)

2. Materials and methods

2.1. Cleanroom

All measurements were performed in a nominal ISO Class 6 cleanroom (i.e. less than 1 million particles per cubic meter). However, our measurements show that the cleanroom met at least ISO Class 4 criteria, i.e. less than 1000 particles with diameter $>0.3\,\mu m$ per m^3. The average air temperature and RH in the cleanroom were $22\,^{\circ}C$ and 45%, respectively, which was maintained throughout the measurements. The cleanroom was separated from the outside air by an airlock. In this airlock, the cleanroom clothing (cleanroom gown with bonnet, powder-free sterile gloves, boots and FFP2 face mask) was put on by every person entering the "isolated side" of the cleanroom. Devices and equipment brought into the cleanroom were thoroughly cleaned from dust in the airlock before they were brought into the cleanroom. The logbook used in the cleanroom was also made of powder-free paper. The cleanroom air was constantly monitored during the tests to ensure that the background air was equal or better than ISO Class 4 conditions. As a rule, only one test person (plus one accompanying person for children and adolescents) and in most experiments maximal three (in very rare and brief cases up to 5) scientists were in the cleanroom. All persons in the cleanroom except the test subject wore a well-fitting FFP2 mask while in the cleanroom.

2.2. Instrumentation

Dried particles (by diffusion dryers as detailed in the next section) with diameters ranging from 0.01 to 0.42 micrometers (in 13 log-equidistant with bin boundaries of: 0.01, 0.0133, 0.0178, 0.0237, 0.0316, 0.0422, 0.0562, 0.075, 0.1, 0.133, 0.178, 0.237, 0.316 and 0.422 μm) were measured with a NanoScan Scanning Mobility Particle Sizer (SMPS, model 3910, TSI Inc.), while those with optical diameters (based on Mie's spherical scattering profiles) between $0.3\,\mu m$ and $10\,\mu m$ (in 16 log-equidistant with bin boundaries of: 0.300, 0.374, 0.465, 0.579, 0.721, 0.897, 1.117, 1.391, 1.732, 2.156, 2.685, 3.343, 4.162, 5.182, 6.451, 8.031, 10.0 μm) were measured with an Optical Particle Sizer (OPS, model 3330, TSI Inc.). A sampling interval of $60\,s$ was chosen for the Particle Size Spectrometers (PSSs). Due to some issues with the SMPS, not all SMPS data for all subjects could be used, while OPS data were available for all subjects. As a consequence, values for the particle size distribution of $<300\,\mu m$ are missing in our database for many children and adolescents (more details presented in Table 1 and Section 2.8).

In addition, an Aerodynamic Particle Sizer (APS, model 3321, TSI Inc., 0.5—$20\,\mu m$) was also used for a large part of the experiments to measure the particle size distribution simultaneously with the OPS and SMPS. We found close agreement between the optical diameters derived from the OPS and the aerodynamic diameter of the APS for $<5.0\,\mu m$ particles (see section S1.1 in the SI). However, the APS detection efficiency was very low for larger particles, which seems to be a problem systematically observed with the APS in previous studies too (e.g. see Pöhlker, et al., 2021, and references therein). For this reason, we did not use the APS data. In addition, we compared the OPS measurements with those made with a GRIMM aerosol spectrometer model 11-D with dolomite dust, glycerol mist with 0.5% NaCl and respiratory particles. The normalized measured concentrations from both spectrometers agreed to within a factor 0.5 to 1.5, a difference that was expected. For the APS, on the other hand, the measured concentrations for particles $>6\,\mu m$ were more than a factor of 10 less than the OPS or the GRIMM aerosol spectrometer model 11-D.

The particle size distributions of large particles were measured using HALOHolo, which is a particle imaging sensor using in-line holography with an effective pixel size of $2.96\,\mu m$ and a $160\,mm$ distance between the two arms (Schlenczek, 2018). Images were

taken with a 6576 × 4384 pixel CCD camera with a frame rate of 6 frames per second. The volume sampling rate was $230\,cm^3\,s^{-1}$. After numerical reconstruction (Fugal, Schulz, & Shaw, 2009) and classification of objects via supervised machine learning, the size, shape and location of particles between 6 μm and a few millimeters could be determined. Under the laboratory conditions used here, the image background is more stable and small particles are easier to detect than those obtained during airborne measurements of atmospheric clouds. The holographic setup was calibrated with NIST traceable calibration glass microspheres from ThermoFisher Inc. in seven different sizes from 7.7 to 50 μm diameter. The particles were released manually into the sample volume where they were visible for about a second as a thin cloud as explained in Schlenczek (2018). The same sample volume was used for the calibration as for the actual measurements. Overall, there were only two bead sizes (7.7 and 20.2 μm) with a deviation of 1.0 μm at maximum, all other particle sizes were well within the tolerance given by ThermoFisher (see SI, section S1.2).

We have also calculated the HALOHolo detection efficiency relative to the near-camera regions. It was found that in a region 2.5–20 mm away from the central plane and 2.5 mm away from the probing volume edges, relative detection efficiency is 87% for 6 μm, >90% for >12 μm, and nearly 100% for >32 μm particles. However, as a compromise between statistical convergence, which requires large sampling volume and uniform detection efficiency for all particle size we have restricted our analyzes to a 60 mm long region in the center of sampling volume (Region of Interest, RoI) . With this the RoI is 14.5 mm wide by 9.6 mm high by 60.0 mm long, which at 6 Hz sampling frequency amounts to sampling rate of $3\,L\,min^{-1}$. In order to calculate representative concentration values for each respiratory activity, we accumulated data from holograms that had at least one particle in the RoI and then divided the total particle count in each size bin by the product of the volume and number of holograms contributed to the accumulated particle count.

Empty holograms were excluded to avoid counting situations in which the subject did not speak/exhale into the sampled volume. It should be noted that due to the strong directionality of the respiratory flows, it was not trivial for the subjects to always target the sampled holographic volume during the entire duration of the measurements, even if the subjects were monitored by an assistant during the entire measurement. Since the holograms can only be evaluated in post-processing, we could not improve further beyond active monitoring. As a result, the empty holograms were designated as "false-zero" holograms, the inclusion of which would have affected the calculated concentration by a factor of 4 to 40 (depending on activity) lower than the values reported here. When only holograms in which a particle was visible in the background filter image were reconstructed (on average, <5% of all holograms), the concentration of particles >30 μm, averaged for a few subjects/activities, was overestimated by ~ 60%, whereas the concentration of particles <15 μm was underestimated by ~ 40%. However, these estimates were not systematically observed in all measurements, so no concrete conclusion could be drawn to correct the data. In any case, the uncertainty that could be introduced by the choice of holograms to be reconstructed is much smaller than the concentration uncertainty that can come from the false-zero holograms. Moreover, the inclusion of holograms with at least one particle within the total probe volume (as opposed to including holograms with at least one particle in the effective sampling volume) would have reduced the concentration of (>9 μm) particles in Fig. 6 by a factor of ~ 2.3, which in any case is within the variability between subjects. Nevertheless, the observed agreement between the measured particle concentration and exhaled diameter with the PSS and HALOHolo supports confidence in the correctness of the analyses and the validation procedure used in processing the HALOHolo data.

For sound pressure measurements we used the 2 Hz PEAKTECH 8005 digital sound-level meter capable of measuring sound levels between 0.1 dB–130 dB at 0.1 dB resolution. Only the sound pressure data that were obtained during the combined holographic and funnel-sampling measurements were used, during which unobstructed sound pressure at a distance of about 20 cm away from the subject was measured. Nonetheless, absolute values reported here should be taken cautiously since the walls of the cleanroom were acoustically reflective.

2.3. Measurement setup

While for holographic measurements respiratory particles were directly imaged at about <5 cm away from the subject's mouth, for PSS measurements the exhale flow was sampled via two different methods: (i) specifically designed full-face mask, hereafter referred to as "isolation-shield", and (ii) a plastic funnel.

In Fig. 1, the different methods of how the exhaled air is sampled for analysis with the PSSs are shown. To sample the exhaled air directly and to minimize mixing with cleanroom air isolation-shields were developed based on snorkel masks. These masks were modified and equipped with adapters. Two different models were used, initially we used the Neuluft Panorama Snorkel Mask (isolation-shield "old") and later due to unavailability of the first the Khroom Sports Seaview X M-1502 (isolation-shield "new"). The masks used had two different sizes to fit best to the subject. A similar design was used in the Pneumask project from Stanford University as alternative PPE for hospitals (https://www.pneumask.org) to create masks for hospitals. Both, the isolation-shields old/new are shown in Figs. 1A and B, 2 and 3A. Both isolation-shields seal to the rim of the face and have an additional sealed barrier between the upper half of the face and the nose and mouth area. For both types of isolation-shields, the clean inhaled air enters the shield through a one-way inhalation valve on top of the shield. The air then passes along the forehead and the eyes and through two one way valves on each side of the nose into the sealed mouth/nose volume. When the subject exhales one way valves close and another one way exhalation valve opens and delivers the air into a buffer volume (marked in light red in Fig. 1). First, we used isostandard medical heat and moisture exchangers (HME filters) on both the inlet and outlet sides (similar to Pneumask project). The inlet filter removed 99.999% of all particles in the inhaled air, and the same outlet filter ensured that no particles were exhaled into the room air. Although the isolation-shields worked very well in an everyday environment with high particle concentrations, it was still beneficial to conduct the experiments in a high-quality cleanroom. It turned out that the isolation-shields did not fit 100% tightly on the face of some subjects. Consequently, in an unclean environment, the aerosol signature of the outside/room air was

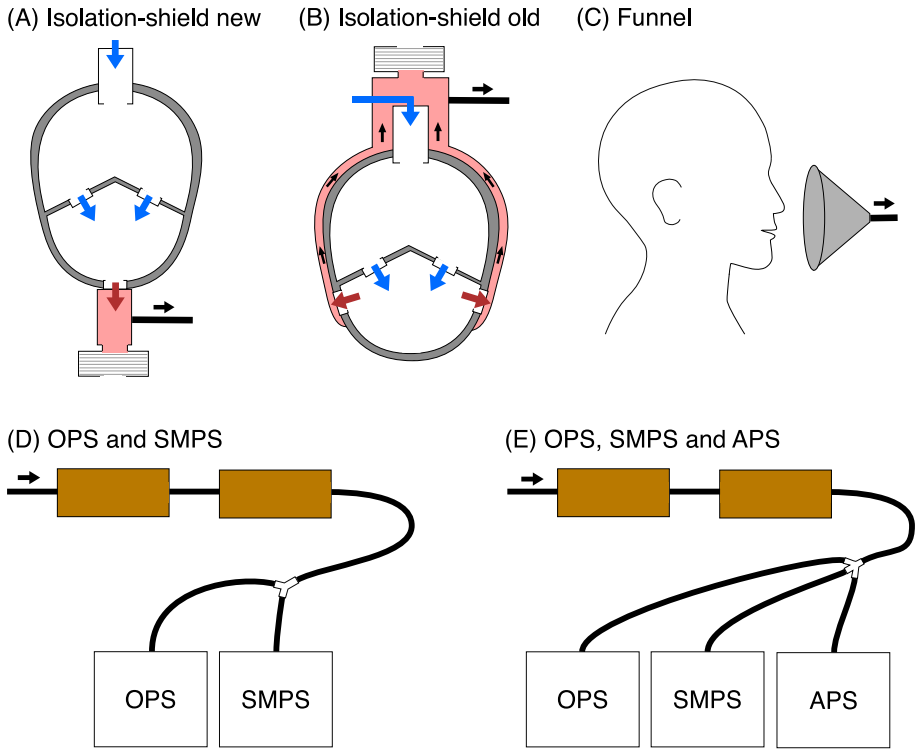

Fig. 1. Schematic of the measurement setups used. First part of the measurement setup: sampling methods. To sample the exhaled air, either (A) the isolation-shield new, (B) the isolation-shield old or (C) a funnel was used. Blue arrows indicate valves that are only open during inhalation, red arrows indicate valves that are only open during exhalation. Shaded red areas represent the exhale buffer volume. The sampling tube (illustrated as thick black lines) is connected to one of the setups (D) or (E). Second part of the measurement setup: the with one of the sample methods (A–C) sampled flow passes through PTFE tubes, two diffusion dryers (illustrated as brown rectangles) and is then analyzed in either (D) OPS and SMPS or (E) OPS, SMPS and APS. (For interpretation of the references to color in this figure legend, the reader is referred to the web version of this article.)

low but visible in the data. For this reason, we felt it necessary to conduct all experiments in the cleanroom. In the cleanroom, these tiny leakages had no significant effect on the measurements due to the extremely low leakage rate of clean air at the seal to the face. During the experiments in the cleanroom, we initially used the inhalation filter, but later we did not. Removing the filter reduced the subjects' work of breathing, while the inhaled air remained clean due to the cleanroom environment. When comparing the tests with subjects with and without the intake air filter, no significant difference was found in the measurements. We also made comparisons of the isolation shields old and new with a number of subjects and found no significant difference in the particle concentrations measured.

With the isolation-shield new (Fig. 1A), the exhalation valve and the buffer volume are located directly on the underside of the isolation-shield. With the isolating shield old (Fig. 1B), the air enters the side channels of the mask and flows upwards into the buffer volume of the adapter — therefore only one filter was used there. In both cases, the exhaled air is sampled with the PSS sampling tube at a constant sampling flow. Since the one-way valve before the exhalation buffer volume closes during inhalation and the instruments sample the buffer volume at constant flow rate, clean air passed through the exhalation filter towards the buffer during the time the subject was inhaling. To avoid the instruments seeing the clean air, the exhalation buffer volume was chosen so that only the exhaled air was measured. With this a continuous sampling of exhale was possible.

In the simplest setup, Fig. 1C, a funnel with 15 cm diameter was held approximately 10 cm in front of the subjects face at the height of the mouth and nose. The funnel was used in combination with the holographic setup, whose measurement volume was placed in between subject and funnel (Fig. 2B). Throughout the whole measurement campaign, different setups were used to make sure the distance between subject and holographic measurement volume was kept at <5 cm. The effectiveness of these arrangements is discussed in Section 2.7.

The sampled air from either Fig. 1(A) the isolation-shield new, Fig. 1(B) the isolation-shield old or Fig. 1(C)the funnel, traveled through (anti-static) PTFE tubing conforming with EN 12115 and passed through two Grimm diffusion dryers model 8913 in series (each 29 cm long with 19 cm outer diameter). The Grimm dryers were filled with silica beads to dry sampled air to RH below 30% (i.e., below the efflorescence RH, see Pöhlker, et al. (2021)) to ensure measured particles are fully dried. The silica beads were replaced with new ones when required. The effect of the diffusion dryers on the relative humidity is shown in Section 2.10

The samples were then analyzed in a combination of spectrometers: Fig. 1(D) TSI Optical Particle Sizer 3330 spectrometer (OPS) and TSI NanoScan Scanning Mobility Particle Sizer 3910 (SMPS) resulting in a sample flow rate of 1.75 L min^{-1} or Fig. 1(E)

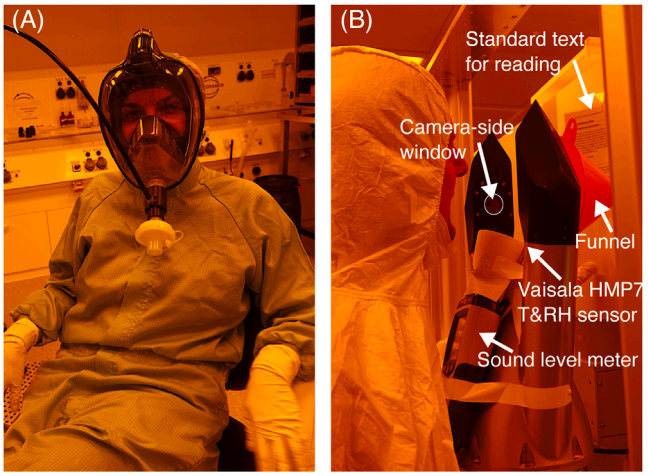

Fig. 2. Photographs of the different sampling strategies. (A) A subject is wearing the isolation-shield new. A HME-filter is on the exhale outlet of the adapter. (B) Example of sampling with the holographic setup and the funnel. The sound pressure level, temperature and relative humidity were measured simultaneously.

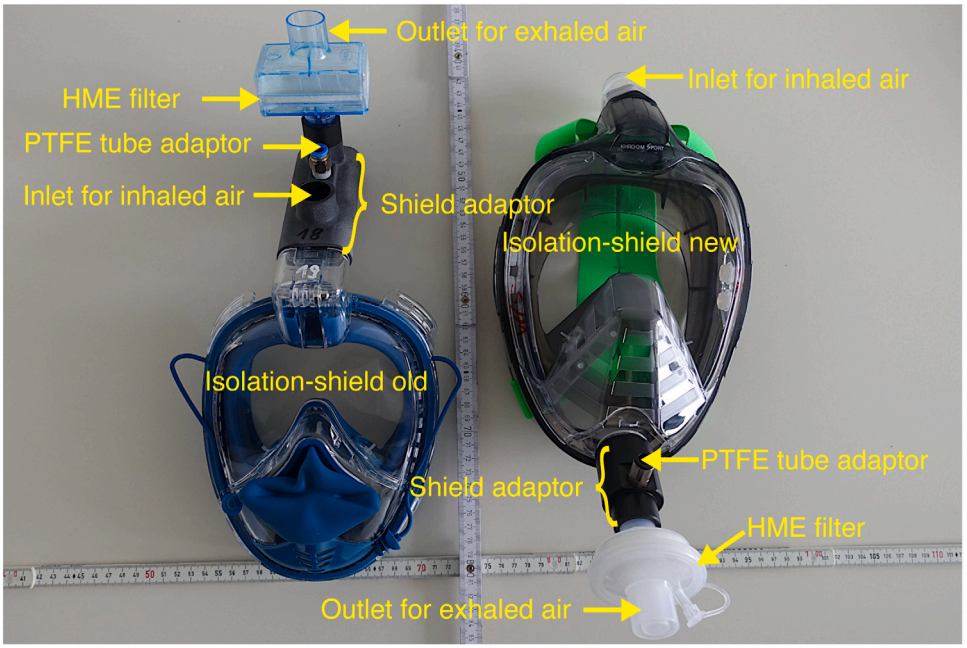

Fig. 3. Top view of the isolation-shields used together with the particle-spectrometry measurements. Photograph of the isolation-shield old (left) and new (right) used for sampling with the respective adapters and exhalation filters attached.

OPS, SMPS and TSI Aerodynamic Particle Sizer model 3321 (APS) resulting in a total flow rate of 6.75 L min^{-1}. The details of the instrumentation are given in the previous section. When two PSS were used, as shown in Fig. 1(D), the tubes were connected via a homemade two-way connector or, in some cases, via the TSI Model 3708 flow divider. When three PSSs were used (see Fig. 1(E)), the tubes were connected via the TSI Model 3708 flow divider to minimize losses due to impaction.

2.4. Subjects

We measured the size spectrum of respiratory particles in exhale of 132 healthy subjects (no acute infection and/or lung disease) aged between 5 and 80 years. The study was approved by the ethics committee of the Max Planck Society. The subjects were recruited in various ways: via the homepages of the Max Planck Institute for Dynamics and Self-Organization (MPIDS), the Department of Infection Control and Infectious Diseases at the University Medical Center Göttingen Georg-August-Universität (UMG), via the

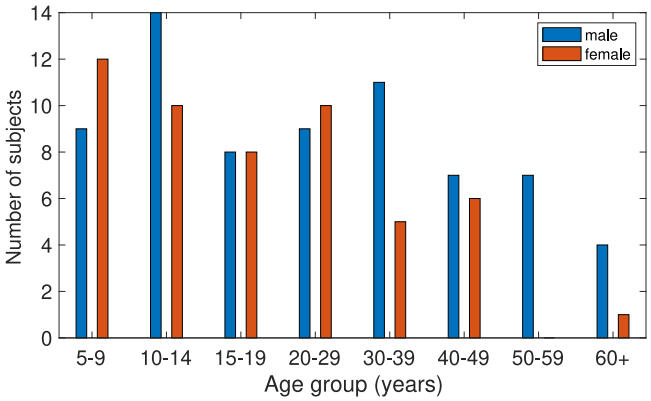

Fig. 4. Distribution of age-groups and self-reported gender of the subjects. (For interpretation of the references to color in this figure legend, the reader is referred to the web version of this article.)

investigators themselves and there were also active requests with the wish to participate that were considered. The data were pseudonymised in accordance with the approved data protection concept and anonymized from the data extraction step onwards.

The age and gender distribution of subjects is shown in Fig. 4. Combined statistics of the subjects, their activities and the instrumentation used is presented in Table 1. All subjects participated voluntarily, were informed in advance about the execution of the experiment and subsequently consented to their participation. The subjects had to be legally competent and not impaired to participate in this study. In the case of children, both the children themselves and their legal guardians gave their consent. Participation could be revoked at any time during the study.

2.5. Respiratory activities investigated

A summary of all respiratory activities discussed in this manuscript is given in Table 2. They were each performed for at least one minute, but typically 5 min for breathing activity and 3 min for vocalization. For the speaking activities, different texts were used, depending on the subject's age and reading abilities. Adults read either the English standard text "Arthur the Rat" (from https://www.york.ac.uk/media/languageandlinguistics/documents/currentstudents/linguisticsresources/Standardised-reading.pdf) or the German standard text "Der Nordwind und die Sonne" plus "Unser Garten" (from Bergauer/Janknecht: Praxis der Stimmtherapie, 3rd Ed.). The youngest subjects were reading the first three paragraphs of the German fairy tale "Die Bremer Stadtmusikanten" (from https://www.familie.de/kleinkind/maerchen/die-bremer-stadtmusikanten-grimms-maerchen).

For singing the subjects were asked to sing "Happy Birthday to You" with names chosen by the subjects themselves, in the key and pitch the subjects felt most comfortable with. Some subjects also selected individual pieces of music or songs for singing after the "Happy Birthday", which we compared against singing "Happy Birthday". For some subjects, we found a slightly higher emitted number concentration for the chosen song in comparison to "Happy Birthday", but the shape of the size distribution was the same and for the average over all subjects, no statistically significant difference could be found.

Our subjects include two professional classical singers (one soprano, one tenor), one professional stage actor and four singers who we would classify as semi-professionals (1 soprano, 1 alto, 2 bass/baritone). All of them performed at least one song selected by themselves (4 classical songs, 2 chorals and 1 pop song). The actor also spoke one of his roles on stage as if the actor was performing on stage. With these additional experiments, we are able to investigate the effect on particle size distribution and emitted number and volume concentration for classical singing versus singing "Happy Birthday", and to investigate possible differences in particle emission between people trained for singing (the professional singers), people trained for speaking (the actor), and the general population (all other subjects). Measurements of particles $>6\,\mu m$ via the holographic setup are available for all singers except for the professional soprano singer. For one semi-professional singer and the actor, we have no isolation-shield data of the selected song/role on stage. The results of the comparison between (semi-) professional singers and other subjects are discussed in Section 3.7.

Besides normal breathing, some other breathing patterns were also investigated on fewer subjects. A common set of breathing patterns done by most subjects was breathing solely through the nose for some minutes, then breathing solely through the mouth. No nose clip could be used for the experiment "breathing through the mouth" due to very limited space within the isolation-shield and we relied on the subjects.

For a set of other experiments, the breathing pattern was synchronized with a "breathing visualization video" showing the deep inhalation up to Total Lung Capacity (TLC) and deep exhalation down to lung's Residual Volume (RV) graphically (from https://www.youtube.com/watch?v=aXItOY0sLRY). This was done at normal speed, double speed, half speed and quarter speed to also investigate the role of the breathing frequency and the total volume flux. The synchronized breathing data are used only to study the effects of breathing rate and frequency, and are not aggregated with the mouth/nose breathing data.

Table 2
Description of the respiratory activities investigated. The so-called *standard activities* done by all subjects were breathing, speaking normal, speaking loud and singing. The rest are referred to as *special activities* and are carried out to understand the origin and production mechanism of respiratory particles.

Activity	Description
Breathing	Normal tidal breathing under relaxed conditions (nose, mouth or both), depth and rate chosen by the subject. Pure nose or mouth breathing is indicated in the data set
Speaking normal	Reading text aloud in a sound volume comparable to conversation in quiet environment
Speaking loud	Reading text aloud in a sound volume comparable to theater performance on stage
Singing	Singing "Happy Birthday" very loudly (fortissimo), tempo, key and pitch chosen by subject
Shouting	Shouting various things (maximum loudness) like "Tor", "Goal" or entire phrases
Coughing	Coughing voluntarily
Deep breath.	deep inhale up to TLC, deep exhale to RV, no breathing for about 1-2 s, followed by deep inhalation to TLC and immediate exhalation to RV
Humming	as "singing", but with mouth closed (humming through the nose)
x s in, y s out	Breathing pattern with x seconds of deep inhalation and y seconds of deep exhalation in sync with the breathing visualization video
1/s exhalation	Breathing to a metronome set to 60 beats per minute, one exhalation per beat
Deep breath. silent	as in "x s in, y s" out for x=10 s, y=8 s
Deep breath. loud	as in "deep breathing silent" but vocalizing "aah" throughout exhale
Airways-closure x s	deep inhale followed by x seconds of holding breath, then exhale to RV and repeat
Wet-lips singing	as "singing" but wetting the lips by tongue in each pause
Lip balm singing	as "singing" but with lip balm (Balea Lippenpflege Sensitive) put on the lips
Lip balm shouting	as "shouting" but with lip balm (Balea Lippenpflege Sensitive) put on the lips
Open-mouth shouting	as "shouting" but mouth kept open with lips not touching each other
Open-mouth singing	as "singing" but mouth kept open with lips not touching each other
Excessive \t\ articulation	speaking the consonant "t" at maximum loudness repeatedly with lips not touching each other

2.6. Measurement procedure

Subjects were investigated one at a time. After wearing the full cleanroom suits, hood and shoes in the cleanroom airlock and entering the isolated side of the cleanroom, first the isolation-shield was adjusted to fit the subject's face properly. We had isolation-shields in two different sizes and took the size that was matching the subject's face best. For a few subjects the seal around the face was not perfect, hence, the leaky parts were filled with lint-free cloth until leak-tight. The tubing, filters and dryers were all replaced with new ones for each subject to minimize the risk of infection and contamination of measurements between subjects. The isolation-shields were reused after autoclaving. The subject typically started with isolation-shield measurements and then went on with simultaneous funnel and holographic measurements. Until the subjects were ready for the first measurements they had already spent a few minutes (~5–10 min) inside the cleanroom. As a result, their lung should have been cleared of non-respiratory-origin particles they could have inhaled in the outside air. Standard activities carried out in sequence with isolation-shield were breathing, breathing through the mouth, speaking normal, speaking loud, singing and humming (activity details can be found in Table 2). Each activity was carried out for 3–5 min at least for isolation-shield measurements. Some subjects were also willing to perform shouting "goal" or its German equivalent "Tor" or various other maneuvers and forced-coughing activities, each for 1 min. The funnel/holographic experiments included reading and singing for about two minutes (shouting and coughing one minute each) excluding breathing activities. In between activities, subjects were allowed to take a break or drink water at will. The entire measurement process took about 45–60 min for each subject.

2.7. Validity of sampling methods

In the following, the sampling methods with funnel and isolation-shield are discussed in more detail regarding potential non-isokinetic sampling and particle losses. At the funnel inlet with 15 cm diameter the sampling air speed is 0.17 cm s^{-1} or 0.64 cm s^{-1} depending on the combination of PSSs for OPS and SMPS (Fig. 1D) or OPS, SMPS and APS (Fig. 1E), respectively. With the funnel setup, no breathing experiments were performed, therefore the exhalation flow can be assumed to be isoaxial. Losses due to impaction and non-isokinetic sampling because of flow direction can therefore be assumed to be minimal. To investigate potential non-isokinetic sampling with the funnel, we need to estimate the exhale air speed at funnel inlet. For this, we measured the exhaled air flow velocity for one subject at mouth height at a horizontal distance of 10 cm with a thermal anemometer probe (Testo 405i). This distance is comparable to the distance between subject mouth and funnel in the setup shown in Fig. 1C. For speaking normal, we found a mean velocity of about 10 cm s^{-1}. This velocity is already in the range of typical turbulent fluctuations in a room. Moreover, we expect the exhale velocity to decrease with distance to the mouth in the cross-section.

With the isolation-shields the sampling is performed directly with the PTFE tube with 8 mm diameter inlet (tube itself has 6 mm inner diameter) from the exhale adapter in a 90° angle to the exhalation flow. The sampling velocity is therefore 58.03 cm s^{-1} and 223.8 cm s^{-1} for the setups in Fig. 1D and 1E respectively. In the isolation shield new, the flow of the exhalation goes through the cylindrical buffer volume (diameter 15 mm) with a speed of 122 cm s^{-1} (based exhalation volume flow rate measurement of breathing with 12.9 L min^{-1}, similar for speaking and even higher for singing). In the isolation-shield old, the flow through the buffer volume is slower as the cross-section is larger but also more complex and likely not laminar due to the complex shape of the flow path through

the mask and the buffer volume adapter. The high exhale flow velocity and the sampling at a 90° angle leads to under-sampling of large particles i.e. particles with high inertia are less likely to follow the 90° redirected flow into the sampling tube. This also shows in the comparison between funnel sampled and isolation-shield sampled data. Whereas for small particles the isolation-shield performed better, for particles >5 μm the particle concentrations measured with funnel were larger and the difference further increased with particle size. We conclude that for small PM5 particles (Particles with $D_0 < 5\,\mu m$, where D_0 is the initial diameter of the respiratory particle in the respiratory tract) the isolation-shield is the best sampling method since we have almost no dilution with surrounding air, for larger particles the funnel performs better due to fewer impaction losses and closer to isokinetic sampling. In all cases, independent of sampling strategy (with PSSs) the long tubes with partially high curvatures and the two dryers are associated with particle losses. For more details on partial losses, exclusions, and corrections, see the following section.

2.8. Considerations of particle size overlap between instruments, particle loss, and instrument deployment

Due to the addition of diffusion dryers on the sampling tubes, it is expected that some particles are lost before reaching the PSSs. To compensate these losses and correct the data, we have performed a series of control experiments in which an OPS measured the particle concentration in a well-mixed room filled with dolomite dust or 0.5% glycerol through diffusion dryers (and tubing), while at the same time another OPS was measuring particle concentration in the room through a tube of similar total length and curvature. The OPSs were first placed in the well-mixed room very close to each other without any tubing to cross-check and correct their measurements against each other in order to ensure they produce similar results once they are in similar conditions. It was found that particle loss in the driers was almost independent of particles size and is about 30% for dried glycerol/NaCl particles and 19% for the dolomite dust, i.e., an average loss of ~ 24%. To correct the cleanroom data for particle loss in the dryers, we multiplied all PSS concentration values by a constant factor of 1.24, which represents the intermediate value between the two limits. The variations associated with using a constant factor instead of a size-dependent correction (± ~ 5%) are much smaller than the within-subject variability.

We have also found that the concentration of dry sub-micron particles, i.e., $D_0 < 5\,\mu m$, in the samples measured with the isolation-shield is on average about 2.6 times higher than in the samples collected via the funnel for the same subject/activity combinations. This we associate with the fact that with the isolation-shield a lower sample dilution with the cleanroom air can be expected than with the funnel, which is achieved by using a *buffer volume* in sampling line of the isolation-shield at least for vocalization activities (more detail is in SI section S1.3). Therefore, data of particles with D_0 <5 μm measured with the funnel gets corrected by the mean ratio of concentrations of those measured with the isolation-shield to those of the funnel. In addition, concentrations of particles >5 μm are corrected with the ratio of concentrations of those measured with the funnel to that of the isolation-shield. We also found that the concentration measured with the isolation-shield and the dryers, on one hand, and measured by directly exhaling into the OPS (and without dryers), on the other, are close to unity for fully-dried <1 μm particles. This indicates that possible electrostatic losses due to the plastic components of the isolation-shields are negligible.

We performed a comparison of the $dN/dlogD_0$ concentrations in the overlapping bins of the TSI SMPS (last bin) and the TSI OPS (first bin). It was found that the concentrations measured by the SMPS are higher than those of the OPS. This discrepancy was expected since, according to calibration certificates of TSI, the detection efficiency of our OPS unit for the smallest bin is 50%, while the largest bin of our SMPS has an efficiency of 90%. After applying the associated detection efficiency, the value of the merged channel was within ~ 14% of the values measured in the last channel of the SMPS. For the overlapping channel, hence, the corrected OPS data was used. This also shows the close agreement between the electron mobility diameter measured with the SMPS and the optical diameter measured with the OPS for respiratory particles.

By using the Particle Loss Calculator (PLC) tool (von der Weiden, Drewnick, & Borrmann, 2009) while taking into account all possible loss mechanisms and using conservative values for inlet aspiration angles and flow rate, and sampling-tube length and angle of curvature/incidence to assess the worst-case sampling efficiency, we found that the total sampling efficiency for <2 μm dry particles (D_0 <9 μm) is >70%, which is an acceptable value. For larger particles PLC estimates a sharp decrease in sampling efficiency due to inertial impaction. This is, in particular, noticeable when comparing the concentration of dry particles larger than 2 μm between the samples collected by the funnel and those collected by the isolation-shield, for which strong inertial loss on the frontal part of the isolation-shield is expected, i.e., the ratio of particle concentration measured by the isolation-shield to that of the funnel is about 1.0 for 2 μm, 0.4 for 3 μm and 0.05 for 10 μm dry particles. Considering all of the above, it is obvious that our PSS data do not capture the true concentration for >2 μm fully dried particles (i.e. exhaled wet diameter D_0 >9 μm, taking into account a shrinkage factor of 4.5, as explained in Section 2.9). As a result, the final aggregated data are obtained by replacing the particle concentration D_0 >9 μm measured by the OPS with the data obtained by the holographic setup.

Furthermore, given the non-uniform age distribution shown in Table 1 (and the empirical model presented in Fig. 7) for the standard activities between SMPS (average median age of ~ 35) and OPS (average median age of ~ 26), estimations of the multimodal parameterization for PM5 particles is associated with ~ 20% uncertainty due to non-uniformity in the age distribution. However, the data is not corrected due to this since the variability within and between subjects is much larger than this uncertainty.

2.9. Particle size shrinkage by evaporation

It is critically important to correct the data to account for particle size shrinkage during measurements, especially for small particles that can shrink significantly within fractions of a second after exhalation. The shrinkage depends on the composition of the particles, the measurement conditions and the time interval between exhalation and measurement. The exhaled particles from the oral cavity primarily consist of saliva, those from the Lower Respiratory Tract (LRT) primarily of Airway Surface Liquid (ASL).

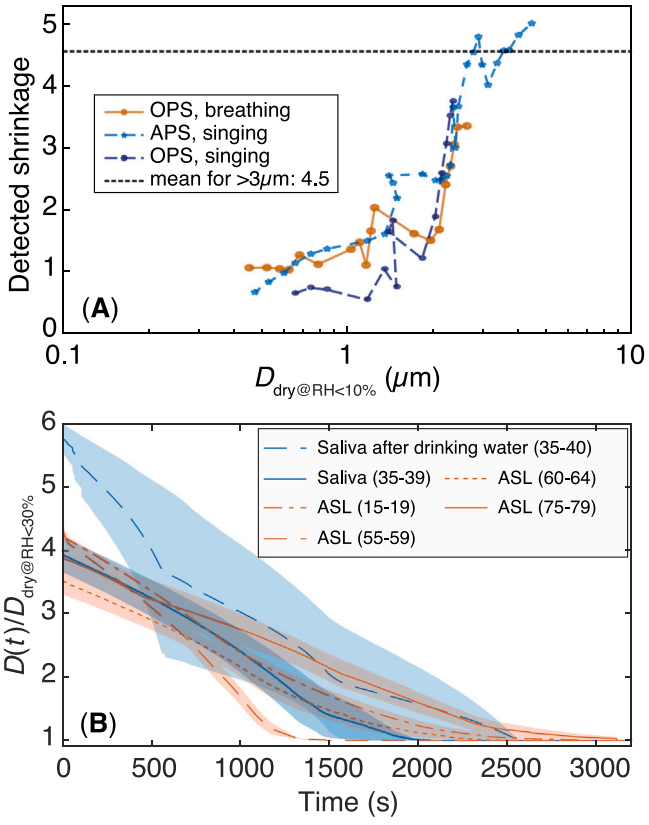

Fig. 5. Shrinkage ratio of respiratory particles and samples from the LRT and URT due to evaporation in a low humidity environment. (A) By calculating the ratio between diameter of particles exhaled by a subset of subjects during breathing/singing without dryers (wet sampling) and the diameter of particles with the same concentration as the wet samples but collected with diffusion dryers (dry sampling at RH<10%); (B) Equivalent spherical diameter of the 9 analyzed saliva and 36 ASL particles as a function of time normalized by the equivalent spherical diameter of the residue. The sample droplets shown in (B) had a diameter of 1–2 mm at the beginning of the drying experiment. Subject 5-years age-range is shown in parentheses in the legend, lines are the mean of samples and the shaded regions visualize the standard error. OPS stands for TSI Optical Particle Sizer model 3330 and APS stands for TSI Aerodynamic Particle Sizer model 3321. Saliva droplets were sampled either after at least 15 min without drinking water or immediately after drinking a sip of water. (For interpretation of the references to color in this figure legend, the reader is referred to the web version of this article.)

Saliva is ~ 99% water mixed with various salts and organic materials like mucins (Pöhlker, et al., 2021). At a solids content of 1% and assuming that the dissolved solids have the same density as water, the shrinkage for saliva droplets is a factor of 4 to 5 at RH<40%, which is in agreement with measurements (Lieber, Melekidis, Koch, & Bauer, 2021; Pöhlker, et al., 2021; Stiti, Castanet, Corber, Alden, & Berrocal, 2022). The airways in the LRT of the adult lung has approximately 23 generations of bifurcations with the trachea being the zeroth generation and the terminal bronchioles number 23. In the LRT, the ASL has two distinct layers depending on the generation: (i) a complex hydrogel mucus layer that is directly exposed to the inhaled/exhaled air and acts as a clearance vehicle and protective barrier against foreign particles and pathogens (up to generation 15–16), and (ii) a periciliary fluid-like layer in which the cilia beat and which up to generation 15–16 is below the first layer (for generation >17 only the periciliary fluid-like layer remains) (Romanò, Muradoglu, Fujioka, & Grotberg, 2021; Song, Cahn, & Duncan, 2020). The primary component of the overall ASL in healthy humans is water, with a nonvolatile solid fraction of approximately 1.1–2.3% *wt* (Anderson, et al., 2015; Hill, et al., 2014). Using these values and assuming that the solids have the same density as water, a shrinkage factor of 3.5–4.5 can be expected for completely dried ASL. This is lower than the swell factor of 6.25 reported for exocytosed airway mucus but it is higher than the value estimated by Nicas, Nazaroff, and Hubbard (2005), which is based on the rather high ~ 9% *wt* solid content taken from the measurements of Effros, et al. (2002). Holmgren et al. (2011) report measurements of exhale particle size distributions measured between 5%–35% and 70%–85% RH and extrapolate assuming pure hygroscopic growth by approximating the ASL by an aqueous NaCl solution. They calculate a shrinkage factor of 2.4 from 99.5% to 75% RH. Recent data of Groth, Cravigan, Niazi, Ristovski, and Johnson (2021), which are based on measurements of cough particles at RH<90% coupled with hygroscopic growth models yield a shrinkage factor of 2.8 at 0% RH. It should be noted that the data measured at high RH shown in Fig. 3 of Groth, et al. (2021) are also consistent with larger shrinkage factors.

Overall, published shrinkage factors vary widely in the data available in the literature. To correct our data measured in the PSSs at an RH different to that of the human respiratory tract, it was necessary to quantify the shrinkage of human saliva and ASL reliably. To this end, we used two independent experimental approaches. In the first approach, exhaled particles were measured

during breathing and singing using PSSs with/without diffusion dryers (i.e., dry/wet) on 11 subjects (200 experiments totaling 370 min of measurements). The shrinkage factor can then be calculated by dividing the diameter of the wet particles by that of the dry particles with the same concentration, with the data shown in Fig. 5A. It should be noted that although the wet measurements were conducted by breathing directly into the inlet of the spectrometer, submicron particles fully dry inside the instrument on their way to the measurement volume thus giving a "false" shrinkage factor of about unity (as seen in Fig. 5A). For larger particle diameters above 2 μm the apparent shrinkage factor for particles produced during breathing grows to 3 and cuts off. The data does not show the plateau one would expect to observe for a "true" shrinkage factor. We attribute this to the particles during breathing being small and influenced by drying in the instrument. However, for singing the data is continued to larger particles >3 μm and plateaus around a shrinkage factor of 4.5. This value is consistent with what is expected for the solid content of saliva and ASL.

In the second approach, we have directly measured shrinkage of human saliva (9 saliva droplets from one subject) and ASL (36 samples from four subjects) as shown in Fig. 5B. ASL samples were collected from four patients via tracheostomy with no respiratory-related diseases, which were examined upon collection to be free of pathogens. Droplets with a diameter of 1-2 mm of saliva and ASL were then suspended each on a single horizontal strand of human hair with mean diameter of 50 μm and let to dry. The relative humidity of the room was ≤ 30% for most experiments (if not explicitly stated otherwise) and the temperature was 23.1 °C to 23.2 °C. This method of suspension ensures that the whole droplet surface is exposed to the surrounding air and the humidity gradient is similar to that around a freely floating droplet, unlike in the case of a drop resting on a (e.g. hydrophobic) surface. In order to prevent air drafts from affecting the evaporation rate, we enclosed the experiment in a large transparent glass box. We recorded the silhouette of the drying droplets using a Phantom VEO4K 990L camera with the optical axis oriented horizontally and perpendicular to the hair. We used an approximate method to measure the droplet size at any time, which rests on the approximation that the cross-section of the droplet in the plane normal to the hair is roughly circular in shape. One can then obtain the droplet volume by simply integrating the squared apparent diameter along the hair length and subtracting the contribution due to the hair itself. The approximation is certainly valid in the initial stages of the drying process, when the droplet equivalent spherical diameter is much larger than the hair diameter, since the droplet was close to spherical (Bond number was at most 0.2). In the later stages, this approximation might break down due to increased effects of impurities and small volume. In order to check the cross-section shape of the dry residual, we rotated the hair to nearly align with the camera optical axis and confirmed that it was indeed typically a nearly circular ellipse. As a further check of the volume-computing method, we selected three dry residuals at random and obtained their convex hulls by rotating the hair with the residual along its axis and recording the silhouette as before. The equivalent spherical diameters of the residuals computed from the convex hulls were 3, −5 and 14% different from those obtained by the circular cross-section approximation.

The mean shrinkage factor for saliva was ~ 4, while it was ~ 5.8 when the subject drank water before sampling. This indicates that depending on the hydration level a high within-subject variability can be expected. ASL shrinkage was found to be in the range of 3.5–4.3. However, it should be noted that the residue-volume extraction method used here tends to underestimate the shrinkage factor and it was measured at a higher RH compared to those of PSSs. Putting both results together a shrinkage factor of 4.5 shown by the dashed line in Fig. 5A is consistent with both experiments and expectations based on dry mass. We used this shrinkage factor, i.e. 4.5, when analyzing the measurement data of the PSSs to back-calculate the fully wet particle size D_0 at the time of exhalation from the fully dried particle diameter at the time of measurement. For data obtained with the in-line holography system, which is based on measurements a few centimeters from the subject's mouth or nose and includes only large particles (D_0 >9 μm), shrinkage can safely be considered negligible.

2.10. The efficacy of the diffusion dryers

The relative humidity inside the particle sampling system was measured with one subject for three standard activities, which were breathing, speaking normal and singing. Between the diffusion dryers and the PSS, a calibrated Vaisala HMP7 temperature and humidity sensor was placed to measure temperature T and relative humidity RH in a distance from the isolation-shield where usually the PSSs would be located. The first experiment was done without diffusion dryer, the second experiment was done with one diffusion dryer and the third experiment was done with the two diffusion dryers used in all measurements. Experiment 1 acts as a reference as it shows what would happen inside the tubing if the sample flow was not dried. Ambient conditions in the cleanroom were T = 21 °C and RH of 44 %. The first observation is that it took 115 s from the start of the breathing experiment until RH changed. Within less than 3 min, RH exceeded 85 %. The maximum RH of 87.5 % was reached 220 s at the end of the breathing experiment. 8 min after the end of the breathing experiment, RH was decreasing rapidly, following an exponential decay. The overall trend did not change when comparing the data from breathing with speaking or singing.

With one diffusion dryer the ambient RH was as low as 12 % and even after 5 min of breathing, the maximum RH observed was 19 %. This experiment shows that even one diffusion dryer reduced the RH in the particle sampling system to the RH of <30 % required for complete drying of the particles (Pöhlker, et al., 2021). In the experiment with the two dryers, the standard measurement setup, the minimum RH was lower, as expected, at 9.45 %.

2.11. Multimodal log-normal fits

Multimodal lognormal regressions of the average data were performed for each of the activities studied. The fits present a good parameterization of the data and thus allow a convenient use by others. Our goal here is solely to parameterize the measured data for each activity. We found the multimodal lognormal regressions to give very good results, although other functional forms or number

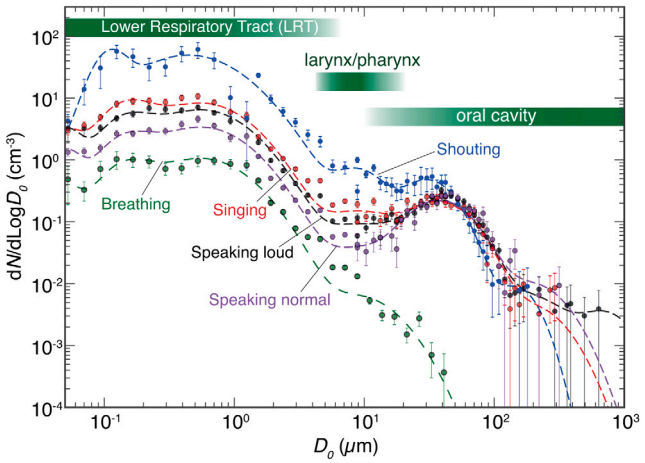

Fig. 6. Measured exhalation particle size distributions versus exhaled particle diameter D_0 obtained from 132 subjects. Particle size distribution from the arithmetic mean of the normalized concentrations over all subjects performing the same activity. The vertical bars show the (symmetrical) standard error. Dashed lines show the multimodal lognormal parameterization for each activity — parameters are shown in Table 3. Horizontal stripes above the curves indicate the inferred sites of origin in the respiratory tract (to be discussed later in Section 3.3). For the smallest and largest particles, i.e. modes 1, 6 and 7 in Table 3, the fit was performed to few data points, some with large uncertainties, and should therefore be interpreted with care.

of modes might also be suitable. For all activities except shouting, the mode diameters and geometric standard deviation were set iteratively minimizing the number of modes required, while the amplitudes were found by minimizing the difference between the regression and the data for each activity. For shouting the modes, geometric standard deviation and amplitudes were allowed to change during the fitting procedure.

3. Results and discussions

3.1. Summary of the main findings

Fig. 6 shows the log-normalized concentration of respiratory particles arithmetically averaged over all test subjects as a function of the exhaled diameter D_0. Fig. 6 is based on subject-specific measurements of size and concentration across the entire size spectrum, from nanometers to millimeters, for breathing and vocalizations. The data constitutes more than 5800 min of particle spectrometry and 12,000 holograms from 132 healthy individuals (56 female, 76 male) aged 5–80 years (mean:25.5 and median 19.0 years) for breathing and specific vocalizations, see Table 1. The shrinkage factor of 4.5 was applied to the fully dried PSS data to calculate back the droplet exhaled diameter before merging it with the wet holography data as explained in Section 2.9. In the following, all particle diameters given refer to exhaled (wet) diameters D_0, unless otherwise stated.

As shown in Fig. 6 the data from breathing and vocalizations differ significantly, i.e., vocalization not only increases particle concentration for small particles, but also the concentration of large particles. The deviation becomes even more pronounced above $D_0 \sim 5\,\mu m$, where particle concentration for breathing decreases rapidly with increasing particle size whereas for other activities it plateaus before increasing. The concentration of $<20\,\mu m$ particles increases with vocal sound pressure also, which agrees qualitatively with previous observations (Alsved, et al., 2020; Asadi, et al., 2019). The largest particles detected with holography across all experiments are 312 μm, 618 μm, 298 μm and 182 μm for speaking normally, speaking loudly, singing and shouting, respectively. It should be noted that the particle diameters measured were well below the detection limit of about 1 cm for the in-line holography instrument used here.

Looking at vocalization at different vocal sound pressures and single subjects (rather than the mean across all subjects shown in Fig. 6), the concentration of 1.5–7 μm correlates with the sound pressure (to be discussed more in Section 3.6). The average of A-weighted-decibels dBA 3rd quartiles measured at a distance of ~20 cm away from the subject are 78.6 dBA, 83.6 dBA, 85.7 dBA and 102.4 dBA for speaking normally, speaking loudly, singing and shouting, respectively. The measured increase of particle concentration with sound pressure we attribute, at least for particles with an exhaled diameter of <5 μm, to the difference in the lung volume used during the inhalation and exhalation and the time gap between them. We do not attribute this directly to the vocal sound pressures themselves or to the larynx/pharynx. The latter is discussed in detail in Section 3.3, where we address the inferred anatomical origins of the exhaled particles in the airways. Interestingly, the particle size distribution between 20 μm–150 μm is very similar for normal/loud speaking and singing. This strongly suggests that the production mechanism is similar and independent of sound pressure. Table 3 shows the parameters found for the multimodal log-normal fits to the subjects-averaged particle size distribution. The increased concentration at 4.6 μm for all activities we attribute to an instrument bias caused by ripples in Mie scattering profiles of the OPS and the choice of bin cut-points, and not to the physics of exhale emissions. Therefore the log-normal fits are intentionally no applied to this bin but to the three-point geometric mean instead.

Table 3
Fit parameters found for different respiratory activities carried out in this study. For each activity the bin-normalized number concentrations is fitted with a multimodal lognormal equation $dN/d\mathrm{Log}D_0 = \sum_{i=1}^{n} A_i \cdot \exp\left(-\left(\ln\left(D_0/d_i\right)/\sigma_i\right)^2\right)$, where A_i [cm^{-3}] is the mode i amplitude, d_i [μm] is the mode i diameter, σ_i is the mode i geometric standard deviation and D_0 [μm] is the particle diameter at the exhalation. It should be noted that the 1*, 6* and 7* modes are fitted to a few data points and/or close to the detection limit of the instruments. Furthermore, data points close to 6* and 7* modes are associated with large uncertainties. Therefore, the presented fitting parameters are only valid for the size range from 50 nm to 1000 μm while considering large uncertainties for >100 μm particles.

Activity	i							R^2
	1*	2	3	4	5	6*	7*	
d_i (μm)	0.05	0.15	0.56	9.0	38	195	700	
σ_i	0.38	0.60	1.0	0.85	0.70	0.70	0.60	
	A_1 (cm^{-3})	A_2 (cm^{-3})	A_3 (cm^{-3})	A_4 (cm^{-3})	A_5 (cm^{-3})	A_6 (cm^{-3})	A_7 (cm^{-3})	
Breath.	0.37	0.76	1.02	0.006	–	–	–	0.96
Speak. norm.	1.26	2.19	3.38	0.04	0.22	0.01	–	0.99
Speak. loud	3.01	4.50	6.43	0.087	0.22	0.006	0.003	0.99
Singing	2.96	7.03	8.27	0.14	0.21	0.004	–	0.99
d_i (μm)	0.05	0.12	0.48	8.8	31	145	–	
σ_i	0.29	0.49	1.12	0.65	0.58	0.35	–	
	A_1 (cm^{-3})	A_2 (cm^{-3})	A_3 (cm^{-3})	A_4 (cm^{-3})	A_5 (cm^{-3})	A_6 (cm^{-3})	A_7 (cm^{-3})	
Shouting	0.91	42.8	43.3	0.63	0.46	0.009	–	0.95

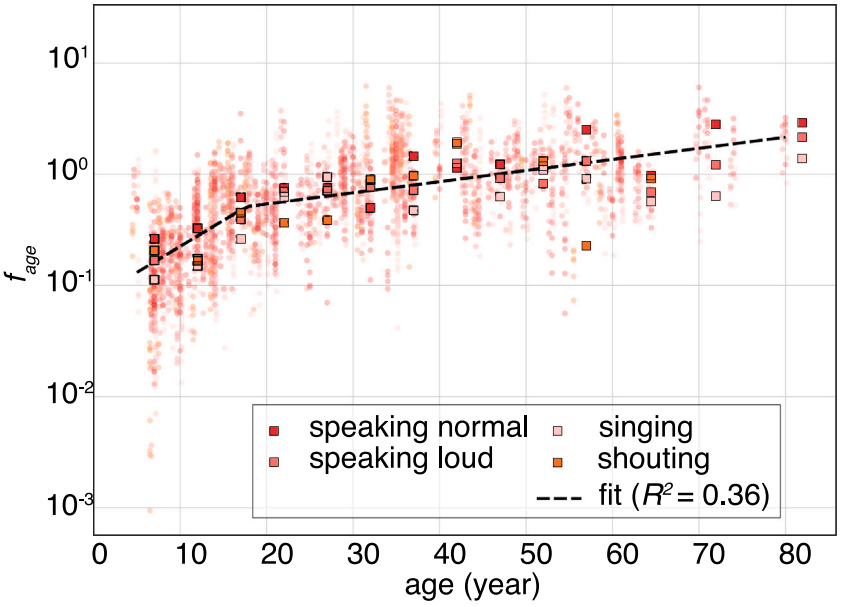

Fig. 7. Dependence of particle number concentration on age for different activities and particle diameter of D_0 = 1.5 μm–5.7 μm. f_{age} is defined as the number concentration produced for a given age group divided by the estimates found by the multimodal log-normal parameterizations provided in Table 3. Squares show the average f_{age} values in 5-year age categories for each activity, while circles, slightly shifted horizontally for each activity for better visibility, show the f_{age} for each individual experiment. The dashed line is a piece-wise linear parameterization fitted to the average f_{age}. The fit provides a multiplier to the multimodal log-normal parameterization to adjust for subject age (in units of year valid for ages between 5 and 80 years): $f_{age} = 10^{0.047\,\mathrm{age}-1.12}$ for under 18 and $f_{age} = 10^{0.01\,\mathrm{age}-0.454}$ for older. (For interpretation of the references to color in this figure legend, the reader is referred to the web version of this article.)

Our data show that biological age is the most important parameter for PM5 concentrations (Section 3.2), whereas gender (SI section S2.1), smoking (SI section S2.2), or exercise habits (SI section S2.3) have no discernible influence on PM5 concentrations. We also could not find a conclusive dependence between BMI and PM5 concentrations (SI section S2.4).

3.2. Age dependence

As shown in Fig. 7, the measured PM5 concentration depends on subject age. We found a dichotomous function for the children/adolescents and adults. While it takes about 7 years for PM5 number concentrations to double in children/adolescents, this increase occurs within 30 years in adults. This observation suggests that most PM5 particles produced during these activities

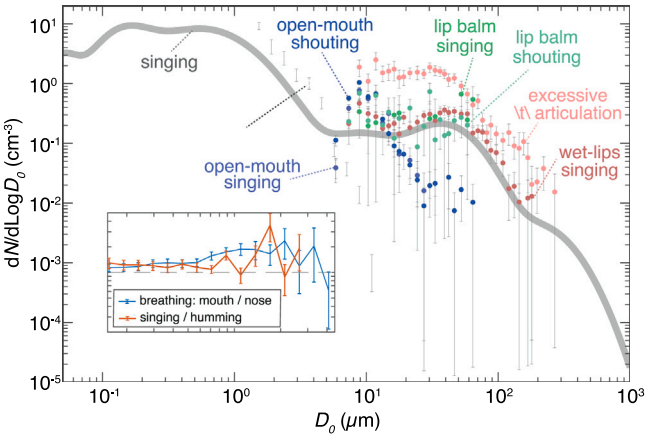

Fig. 8. Bin-normalized particle size distributions for singing and other *special* respiratory activities. Full definition of all activities are presented in Table 2. The thick gray line shows the multimodal parameterization for singing. The inset shows the ratio of total particle concentration as a function of particle diameter between mouth-breathing and nose-breathing, and between singing and humming. The vertical bars show the (symmetrical) standard error. (For interpretation of the references to color in this figure legend, the reader is referred to the web version of this article.)

are generated by the mechanism of airway closure/re-opening, which is known to be age-dependent (Bake, et al., 2019). In contrast, PM5 number concentration during tidal breathing was not observed to depend on age (not shown in Fig. 7), suggesting that children and adults use an equivalent relative lung volume, i.e., not all lung volume is used for respiration and thus airway closure/re-opening and with it the PM5 number concentration is similar for all ages.

Based on the piece-wise linear parameterization shown in Fig. 7, the PM5 number concentrations in exhaled air of children aged 5 years during vocalizations are on average 13% of the mean determined for all subjects, while the PM5 number concentration in exhaled air of 80-year-old persons is 2.1 times the mean. It must be noted, however, the average PM5 volume concentration in children/adolescents is about 0.42 for breathing and 0.38–0.50 for vocalizations compared with the mean of the whole population, while for adults these ratios vary between 1.42–1.68. This indicates that the amount of PM5 emitted by children/adolescents is about one-fourth to one-third of that produced by adults. We also find that the normalized PM5 number concentration at age 45 years is close to unity, showing that our multimodal parameterizations are best at predicting PM5 concentrations at this age. Depending on the activity, the correlation with age gradually disappears for particles with D_0 beyond 5–8μm.

3.3. Origin of the exhaled particles within the respiratory tract

Carefully selected activities, see Fig. 8, that included or excluded specific parts of the respiratory tract show that PM5 particles originate from the Lower Respiratory Tract (LRT), whereas D_0 ~5–15 μm particles originate primarily from larynx/pharynx and D_0>15 μm particles primarily from oral cavity.

As already shown in Fig. 6, the LRT origin of PM5 is supported by the similar shape of the particle size distribution for different activities in this size range. Furthermore, the equivalence in particle concentration between pure nasal and pure oral breathing (R^2 > 99% and p < 0.01, see inset of Fig. 8) renders the oral and nasal cavities unlikely as the origin of PM5. In addition, while breathing the vocal cords are inactive and shear by flow is low — thus they will not contribute to particle production. In Fig. 8 it can be seen that during deep breathing and singing, we found the same high PM5 concentrations, indicating LRT potential as a PM5 source (also see SI section S2.5). The strong increase in particle number concentration during deep breathing is likely associated with the subject reaching the point at which extensive airway closure occurs, which was also reported in several other previous studies (see Bake, et al., 2019, and references therein). The increased PM5 concentration with age also supports the role of the LRT (Section 3.2) as it is well known that with increasing age airway closure occurs earlier, i.e. at lower lung volumes (Bake, et al., 2019).

We also found that the breathing frequency does not influence the exhale particle size distribution (SI section S2.6). Furthermore, pausing between full inhalation and exhalation significantly decreased particle emission similarly to observations reported previously (Holmgren et al., 2011; Johnson & Morawska, 2009) (SI section S2.5). We conclude from these observations that PM5 particles during breathing originate predominantly from the LRT, i.e., the lung, and their concentration is not a function of breathing frequency, but rather of the lung volume used and the pause between inhalation and exhalation.

Now the question arises from which part of the respiratory tract the PM5 particles originate during vocalizations. Surely some of these particles are produced in the LRT similarly to breathing, since the subjects not only vocalized but also had to breathe. Thus, also during singing and shouting the LRT must be a major PM5 contributor. But what is the influence of the remaining respiratory tract? The similarity in particle size distribution between humming the "Happy Birthday" song with mouth closed and singing the same song shown in the inset of Fig. 8 suggests that PM5 are not produced in the oral cavity during singing. This leaves the larynx and pharynx as the remaining candidates next to the LRT.

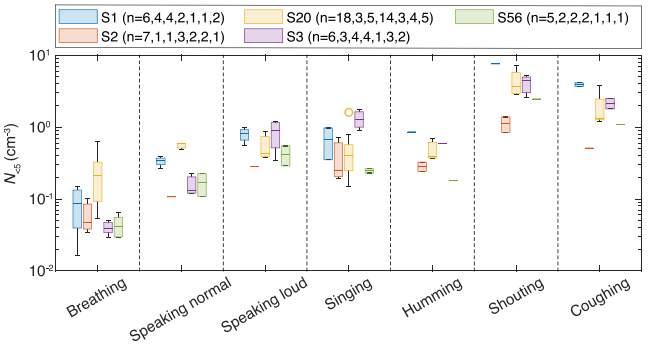

Fig. 9. Within-subject variability for the five subjects with the highest number of independent measurements in the standard activities for both $N_{<5}$. The number of independent measurements n can be found in the legend for each subject in the order: breathing, speaking normal, speaking loud, singing, humming, shouting, coughing. Only measurements where sampling was performed with either the isolation-shield new or old are considered. (For interpretation of the references to color in this figure legend, the reader is referred to the web version of this article.)

Although there is a weak correlation between PM5 concentration and subject sound pressure during vocalization (Section 3.6), which would support the assumption that the larynx is a PM5 source, the large scatter in the data observed suggests strongly that the larynx/pharynx is not a major source of PM5 production. We also found no significant difference in particle size distribution between breathing with and without vocalizations at fixed exhalation flow rate and lung capacity (Section 3.6). Finally, the dependency between PM5 concentration and subject age (as shown in Section 3.2) is consistent with the LRT being the main origin site for PM5. From these observations, we conclude: PM5 particles are predominantly produced in the LRT for all of the activities studied here, while in vocalizations a small contribution to the PM5 concentration will come from the larynx/pharynx (see Section 3.6).

Particles >5 μm are mostly produced during vocalization, so the likely sites of origin are the pharynx/larynx, nasal cavity and oral cavity. This is supported by the fact that we could not detect any >6 μm particles (i.e., the Nyquist detection limit of holographic setup) while measuring nose/mouth breathing at different exhalation flow rates and lung volumes, and humming maneuvers. When singing and shouting with the mouth wide-open, which should eliminate lip contributions, we found that the larynx/pharynx was very effective in producing ~5–15 μm particles, with the mode being around 10 μm. The higher particle concentration during open-mouth singing compared with normal singing suggests that during normal singing some of the particles produced by the larynx/pharynx are removed by inertial impaction on the lips before exhalation. This observation is also consistent with the increase in concentration of particles in the size range ~5–15 μm visible in Fig. 6 during shouting, where the mouth is generally held open longer than during other activities. These observations suggest that the larynx/pharynx is the major producer of ~5–15 μm particles.

The sharp concentration drop at 15 μm for singing and shouting with the mouth open indicates that the majority of >15 μm particles detected for standard vocalizations are produced by the tongue, tongue–teeth interactions and lips. An example of particle size distribution produced only by the tongue–teeth can be seen in open-mouth sound \t\ articulation that leads to production of a wide range of particles mostly >10 μm. Singing while frequently wetting lips with the tongue lead to a particle size distribution similar to singing normally with higher concentration for >10 μm particles, suggesting particles produced by the lips span a wide range of sizes too. However, the main contribution from lips becomes evident for the singing and shouting experiments when subjects applied non-wetting lip balm to their lips. Applying non-wetting lip balm was shown earlier to temporarily hinder formation of saliva filaments between the lips and reduce particle emission (Abkarian & Stone, 2020). Fig. 8 shows that applying non-wetting lip balm is effective mostly for reducing emission of >75 μm particles. Taking all these observations together, the most important points of origin can be derived as a function of particle size, shown as horizontal green stripes at the top of the Fig. 6.

3.4. Variability within and between subjects

3.4.1. Within-subject variability

The within-subject variability is shown in Fig. 9 only for five subjects with the highest number of total independent measurements to visualize this variability. The variability in PM5 particle number concentration spans up to one full order of magnitude. When comparing the within-subject variability for different activities and subjects in Fig. 9, the different numbers of independent-tests n have to be taken into account. The independent measurements of these subjects were performed over the span of 200 days, but some also on the same day. The exhaled particle concentration of each subject can vary as much in a single day as it does over a longer time span up to over 200 days.

For Subject 20 (S20), the number of experiments for breathing and singing was large enough to determine the distribution type. In case of $N_{<5}$ for breathing (18 experiments), we could fit a Gaussian distribution with $\mu = 0.206\,\mathrm{cm}^{-3}$, $\sigma = 0.164\,\mathrm{cm}^{-3}$ and $R^2 = 0.937$, and for singing (14 experiments), we could fit a Gaussian with $\mu = 0.392\,\mathrm{cm}^{-3}$, $\sigma = 0.205\,\mathrm{cm}^{-3}$ and $R^2 = 0.967$. The other activities and subjects did not contain enough experiments for a reasonable fit. Both Gaussian distributions we could fit to the data are relatively broad, which means that the standard deviation is 50% of the arithmetic mean value or more than that ($\sigma/\mu = 0.796$ for S20 breathing and $\sigma/\mu = 0.523$ for S20 singing).

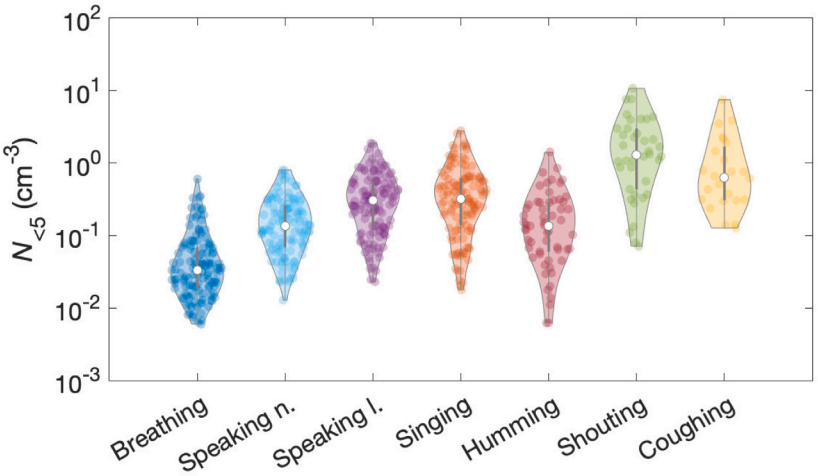

Fig. 10. Between-subject variability for the standard activities. The scatter in exhaled number concentration $N_{<5}$ of PM5 particles is shown via a violin plot. If subjects performed more than one experiment per activity the mean is shown. Only measurements were sampling was performed with either the isolation-shield new or old are considered. The plot was made with Bechtold (2016).

3.4.2. Between-subject variability

The between-subject variability for the standard activities is shown in Fig. 10 (per bin data are shown in SI section S2.7). PM5 number concentration differs between the lowest and the highest emitter by a factor of 100–150, depending on the activity. However, for 90% of subjects, PM5 number concentrations are within 0.05–3.5 of the population arithmetic mean, regardless of activity. While the ratio of PM5 number concentrations when breathing for the highest emitter (one of 132 subjects) to the arithmetic mean of the population is about 10, this ratio is 4.2, 4.8, 5.7 and 5.0 for normal speaking, loud speaking, singing and shouting, respectively. Only 2 out of the 132 subjects were one standard deviation above the mean in $\log(N)$ in all four activities — breathing, speaking normal, speaking loud and singing. For vocalization activities, all emitters with the lowest 5th percentile PM5 concentration were younger than 15 years, and the majority ($> 50\%$) of emitters in the 95th percentile were older than 44 years. The mean (min/max) PM5 volume concentrations ($D_0 = 1.35 - 5.55$ μm measured by the OPS, of which data are available from most subjects) in units of $\mu m^3\,cm^{-3}$ are 0.63 (0.02/7.25), 1.68 (0.02/8.14), 3.45 (0.01/18.92), 4.46 (0.07/22.13) and 15.87 (0.04/70.59) for breathing, speaking normally, speaking loudly, singing and shouting, respectively. Therefore, the pathogen emission from the lungs, which scales with particle volume, can vary by a factor of several hundred to several thousand, depending on the characteristics of the subject.

When comparing the between-subject variability for different activities (Fig. 10) the different number of subjects that performed each activity has to be taken into account. As shown in Section 3.5, we found a log-normal distribution for $N_{<5}$ and $V_{<5}$, which is the reason for presenting the *geometric* mean and standard deviation in Table S3 in the SI. While cumulative quantities like $N_{<5}$ and $V_{<5}$ were always non-zero for the entire cohort of subjects and all experiments, this condition is not necessarily fulfilled for N in individual size channels of the particle size spectrometers. Because of that, we could only investigate the distribution type for $N_{<5}$ and $V_{<5}$ and not for each size bin individually and when particle size distributions are investigated the arithmetic mean was used (e.g. Fig. 6). The arithmetic mean and standard deviation as well as the ratio of standard deviation and mean are given in Table S4 of the SI for completeness and to also give a more intuitive measure of the scatter of the data.

3.5. Total number and volume statistics and the question of super-emission

From all experiments, we investigated the distribution of total PM5 number concentration $N_{<5}$ and total PM5 volume concentration $V_{<5}$ among the subjects. If a subject did multiple experiments of the same kind, the median of $N_{<5}$ and $V_{<5}$ from all experiments of this subject was taken. For both the entire cohort and for each age group as described below, we found that $N_{<5}$ and $V_{<5}$ could follow both Gaussian or log-normal distributions as the quality of fit measured by R^2 was above 0.9 for both distribution types. However, a log-normal distribution in all cases is the better representation of the data compared to a Gaussian, in particular for the tails of the distribution. We calculated the geometric mean μ_g and the geometric standard deviation σ_g for $N_{<5}$ and $V_{<5}$ for each kind of experiment and computed a log-normal distribution with the same μ_g and σ_g. The log-normal distribution was then compared with the measured distribution by performing a two-sided Kolmogorov–Smirnov test. In all cases, the null hypothesis could not be rejected at 95% significance level, which means that the observed distributions can be approximated well by log-normal distributions. In addition, we fitted log-normal distributions to the data and obtained good fits ($R^2 \geq 0.91$) with very little deviation in μ_g and σ_g from the values computed directly from the data. An overview of the results from the fits for the total PM5 number concentration is shown in Table 4.

Table 4
Geometric mean μ_g in cm^{-3} and geometric standard deviation σ_g of $N_{<5}$ for each age group in all four activities obtained from a log-normal fit to the data.

Age	Breathing		Speaking n.		Speaking l.		Singing	
(year)	μ_g	σ_g	μ_g	σ_g	μ_g	σ_g	μ_g	σ_g
5–9	0.024	1.781	0.041	1.654	0.072	1.859	0.068	2.675
10–14	0.020	2.128	0.077	2.324	0.120	2.187	0.129	2.769
15–19	0.022	1.847	0.137	1.594	0.220	1.938	0.220	2.383
20–29	0.027	2.398	0.131	1.704	0.314	1.756	0.391	2.184
30–39	0.043	1.966	0.140	1.916	0.401	1.486	0.428	1.803
40–49	0.050	2.921	0.233	1.611	0.560	1.588	0.605	2.171
50+	0.091	2.879	0.313	1.964	0.571	1.938	0.578	1.872

Table 5
Number of low and super-emitters in the different age groups. n_{sub} denoted the number of subjects for this analysis per age group. The last two columns show how many subjects were low- or super-emitters in all four considered activities.

Age	n_{sub}	Breath.		Speak. norm.		Speak. loud		Singing		In all act.	
(year)		low	high	low	high	low	high	low	high	low	high
5–9	18	3	2	5	4	3	2	3	3	0	0
10–14	25	3	4	4	6	2	3	4	4	0	1
15–19	14	2	3	2	1	4	3	3	2	0	0
20–29	20	4	4	3	3	1	3	2	4	0	1
30–39	15	2	2	1	3	2	3	3	3	0	0
40–49	13	2	3	2	2	1	3	3	2	1	0
50+	21	4	2	2	4	3	3	4	3	0	0
Total	126	20	20	19	23	16	20	22	21	1	2

As there is an age dependence in $N_{<5}$ (Section 3.2), we needed to examine the distribution of emitted $N_{<5}$ among the subjects in subsets defined by age. The strongest increase of $N_{<5}$ as a function of age was seen for subjects below 20 years (also evident in Fig. 7), so we decided to subdivide the data pool in 5 year age intervals from 5 to 19 years, and in 10 year age intervals for the adults of age 20 years or more. The last age group in Table 4 contains all subjects between 50 and 80 years as the total number of subjects in this age category was too small to justify smaller age subgroups. As already discussed in Section 3.2, we see an increase in the geometric mean of $N_{<5}$ with age, which is strongest for the louder phonetic activities (loud speaking and singing).

The numbers of low- and super-emitters (having N one σ_g lower- or higher than μ_g, respectively) in the different activities, as well as the number of low- and super-emitters in all categories, are presented in Table 5. It was found that on average only about 0.8–1.6% of the subjects tend to be either "global low-emitters" or "global super-emitters" in all four activities examined. Between the global super-emitter and the global low-emitter, the span in emitted N can be as much as 6 σ_g if age dependence is ignored.

The percentage of super-emitters in one activity is between 15.9% (breathing) and 18.2% (speaking normal), the percentage of low-emitters per age group and activity is between 12.7% (speaking loud) and 17.4% (singing). With an average of 16.7% for super-emitters and 15.3% for low-emitters, both extremes are nearly equally distributed within the population. What we also found is that 11/20 (55%) of the low-emitters in breathing are also low-emitters in at least one phonetic activity, and 10/20 (50%) of the super-emitters in breathing are also super-emitters in at least one phonetic activity. The abundance within the examined population of the super-emitters in breathing plus one phonetic activity is 8.0% and the abundance of low-emitters in breathing plus one phonetic activity is 8.4%.

3.6. Influence of vocal sound pressure and pitch

The A-weighted-decibels dBA 3rd quartiles measured at a distance of ~20 cm away from the subject for vocalization activities averaged over all the subjects are 78.6 dBA, 83.6 dBA, 85.7 dBA and 102.4 dBA for speaking normally, speaking loudly, singing and shouting respectively. This suggests that the elevated particle concentration observed for PM5, as an example, from speaking loudly to speaking normally is most likely due to an increase in vocal sound pressure. We have observed a connection between loudness and being a low-emitter or a super-emitter. For speaking normal, we found a mean of the loudness 3rd quartile of 77.6 dB(A) in the cohort of the low-emitters, and 82.7 dB(A) in the cohort of the super-emitters. The difference between the two cohorts, however, is not significant ($p = 0.083$). For speaking loud, we found a mean of the loudness 3rd quartile of 81.1 dB(A) in the cohort of the low-emitters, and 89.5 dB(A) in the cohort of the super-emitters, which is a significant difference between the two cohorts ($p = 0.006$). The biggest difference was found for singing with a mean of 3rd quartile loudness of 81.2 dB(A) in the low-emitters and 92.0 dB(A) in the super-emitters, which is also significant ($p = 6 \cdot 10^{-5}$). So the difference between low-emitters and super-emitters in the phonetic activities can at least partially be explained by the loudness.

However, each subject had – among other variable parameters, such as age – a different increase in sound pressure from normal to loud speech or to singing. To remove the subject-dependent part, we reanalyzed the data by considering only the 76 subjects aged 5–75 years, all of whom performed speaking normally, speaking loudly and singing as shown in Fig. 11. For these subjects we found

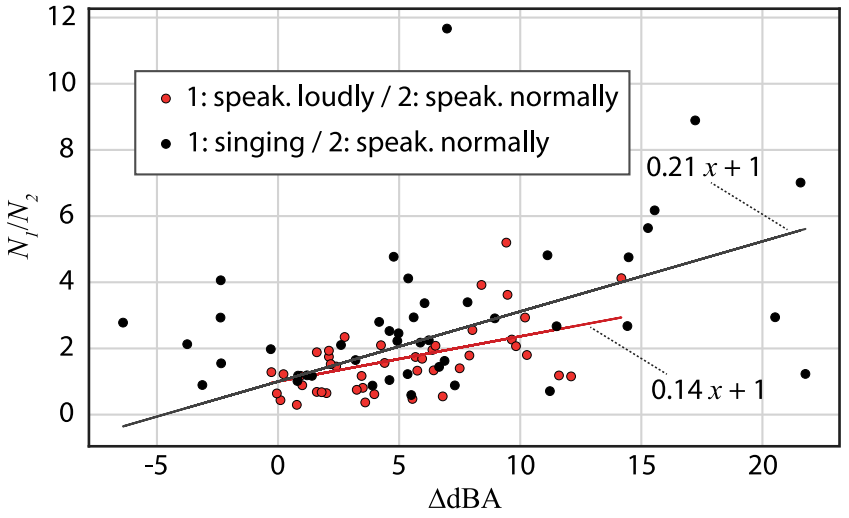

Fig. 11. Impact of change in sound pressure on concentration of particles with 1.5 μm< D_0 <7 μm for the same individual when singing or speaking loudly, normalized by particle emission during speaking normally. Each circle reprsents an individual subject. (For interpretation of the references to color in this figure legend, the reader is referred to the web version of this article.)

that there still remains a significant correlation, i.e. $p < 0.01$, between the concentration of 1.5-7 μm particles and sound pressure. A maximum correlation of $R^2 = 0.51$ between sound pressure and particle concentration is found for particles with D_0 ~2.5 μm. There is, however, a significant scatter in the data, which lead to low R^2 values between the linear regression and the measurements. Furthermore, the change in the particle concentration is well inside the within-subject variability for a fixed activity (see Section 3.4).

To isolate the possible PM5 contribution from the larynx and pharynx during vocalization from the influence of ventilation rate, we measured PM5 using the isolation-shield new and OPS for deep breathing experiments with 2 subjects with and without vocalization, i.e. “deep berating silent” and “deep breathing loud”. The silent case is a deep breathing activity synced to a breathing visualization video, whereas the loud case is with a vocalization of “aah” during the whole exhalation of the same breathing pattern without lips/tongue movements (cf. Table 2). Breathing frequency was kept constant over the silent and loud breathing activity since it was synced to the breathing video and in both cases the exhale was a full exhale. Fig. 12 shows the ratio of the exhaled particles during the activity with and without vocalization for both subjects individually and the mean. The vocalization on the exhale does not show a significant difference, in particular for D_0 <3 μm where strong statistical convergence could be achieved. This experiment shows that the PM5 contributions from the larynx/pharynx (if any) are not as strong as those from the lungs during deep breathing. As it is visible from Fig. 8, the number of particles produced during deep breathing is significantly higher than that of most vocalization activities. Therefore, possible influence of larynx/pharynx are not easily detectable in these experiments.

To further elucidate the role of larynx/pharynx on PM5, we have performed a series of experiments on one subject at different combinations of voice frequency and pitch. However, the subject’s ventilation rate was not measured but breathing frequency was synchronized with the breathing visualization video described in Section 2.5. The subject inhaled in sync with the breathing visualization video at 0.5x speed (5 s inhalation, 4 s exhalation, no pause in between) and sung the vocal “A” at constant pitch during the exhale period. Loudness was aimed to be close to the maximum possible for the given pitch. Before and after the singing experiments, two breathing experiments were done for comparison. The sound pressure was measured in C-weighted decibels with the previously described PeakTech 8005 sound level meter, which was placed 1 meter away from the subject’s mouth. Here, the C-weight was chosen to have a more uniform weight across the whole frequency range as the subject started at low A-flat (104 Hz) and continued all the way to treble F (694 Hz). In addition, the audio was recorded via a miniDSP Umik-1 microphone logging to a computer (audio was saved as 24 bit stereo wavesound files). The spectral analysis of the recorded audio was used to verify the pitch measured with the tuner app “CarlTune” on a smartphone next to the subject. Due to acoustic reflectivity of the cleanroom walls and other acoustical issues, we decided to show the median of the measured sound pressure minus the median sound pressure of the cleanroom background. To estimate the relative lung volume used in vocalizing different pitches, the subject sang a given pitch on vocal A until he was out of breath. The “pitch frequency Hz:duration in seconds” results to exhale 3 L are: 104 Hz:25 s, 131 Hz:18 s, 174-265 Hz:15 s, 344 Hz:13 s, 437 Hz:12 s and 522 Hz:11 s. It can be seen that with the increase in the pitch frequency, the used lung volume increases too. Each tidal-breath of the subject lasted about 20 s with the exhaled volume of 1.5 L. Maximum vital capacity of the subject, measured by spirometry at the University Medicine Göttingen, is 4.16 L.

The measured particle size distributions (data from OPS) from this subject are shown in Fig. 13. For singing a certain pitch on vocal “A” at a sound level close to the maximum the subject could deliver, we see a strong dependence of the emitted particle number and volume concentration on the sound pressure. More than 85% of the variance can be explained by this alone. If we also consider a pitch dependence, which can be linear or quadratic, the regression improves to $r^2 = 0.96$ when a quadratic pitch

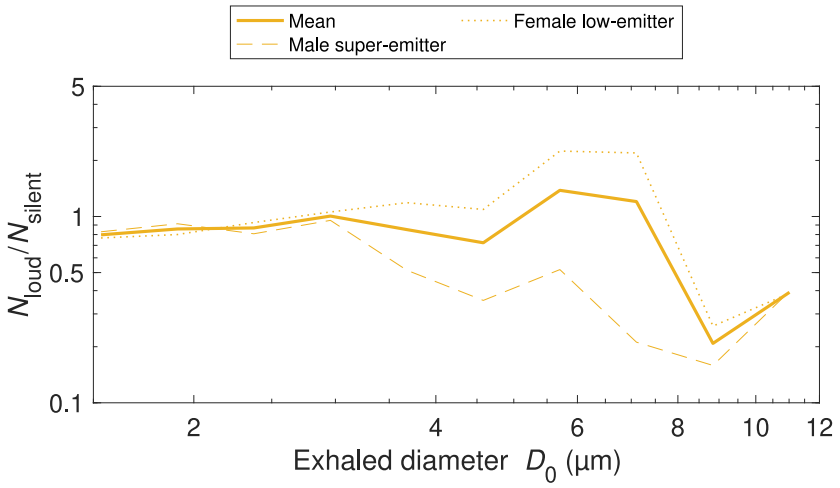

Fig. 12. Effect of vocalization during deep breathing on particle size distribution. Subjects vocalized "aah" during exhalation. Solid lines show the mean over the two subjects. Results for individual subjects are shown in dotted lines as a measure of uncertainty.

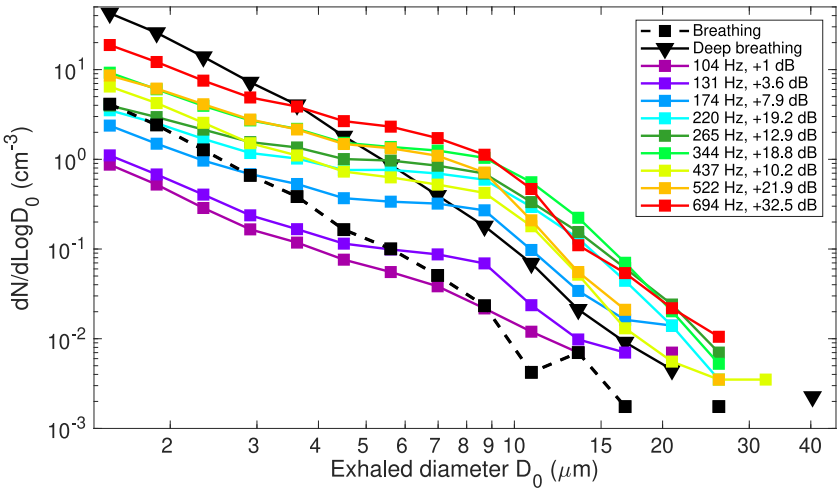

Fig. 13. Particle size distributions measured by the OPS for normal breathing (black dashed line and black squares), deep breathing (black solid line and black triangles), and singing vocal "A" at different pitch (colored lines and squares). For each experiment, the fundamental frequency and the loudness in dB(C) above background level in the cleanroom are given. (For interpretation of the references to color in this figure legend, the reader is referred to the web version of this article.)

dependence is assumed in addition to the linear sound pressure dependence. Taking into account the exhalation duration measured on the subject for a given pitch/exhalation volume and tidal breathing, the trend seen in Fig. 13 can also be largely explained by the lung volume used. An interesting result is that tones ≤131 Hz generally lead to lower particle emission compared to breathing, which can also be explained by the lower exhalation rate of the subject during these activities compared to breathing.

Nevertheless, the difference in the slopes of the particle size distribution between vocalization and breathing suggests that there is some influence of vocalization on PM5 concentration. However, this influence is not as strong as that we observed due to subject age or within-subject variability, or at least it does not contribute significantly to the total emitted volume. Another finding from Fig. 13 is the strong deviation in slope and shape of the curves between vocalizing and breathing at 10 μm measured with the OPS. This is a confirmation of the OPS/in-line holography results presented in Section 3.3, where we found evidence that the larynx/pharynx is the main source of particles with D_0 of 5–15 μm.

Overall, it cannot be reliably concluded that the increase in sound pressure is accompanied by an increase in particle emission for the same exhaled volume. While there are correlations between sound pressure/pitch of voice and PM5 number concentration in some of the results presented above, there is a much stronger correlation with exhaled volume in all cases studied. Thus, we conclude that the influence of larynx/pharynx on PM5 production, if at all, is not as significant as the contribution of the lungs. Without knowledge of actual inhalation and exhalation flow rates and respiratory parameters such as TLC, etc. for each individual, it is not possible to fully quantify the influence of larynx/pharynx on PM5.

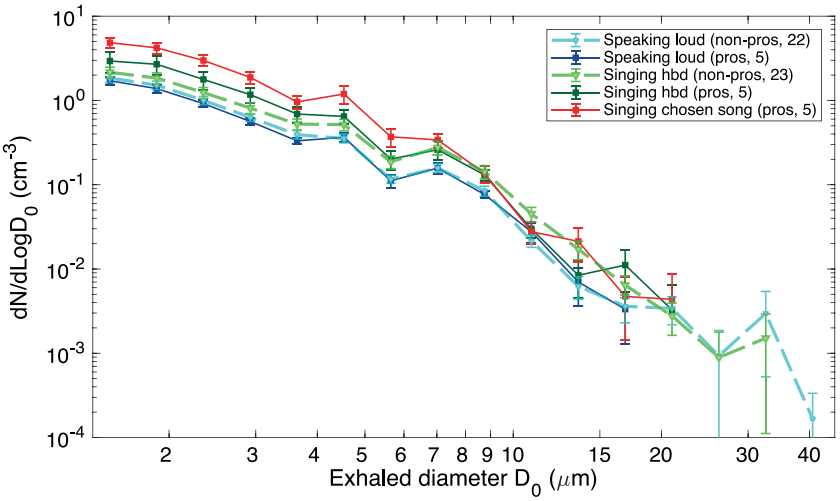

Fig. 14. Particle size distributions measured by the OPS from "non-pros" (i.e. the subjects without professional singing experience, data shown as triangles and dashed lines) and "pros" (self-declared semi-professional and professional singers, data shown as squares and solid lines) for "speaking loud" (blue shades), "singing hbd" (green shades), and singing a specific song (red). The number of subjects is given in parenthesis. Shown are size distribution mean and standard error. (For interpretation of the references to color in this figure legend, the reader is referred to the web version of this article.)

3.7. Influence of (semi-) professional singing skills

When investigating the data measured by the holographic setup, we find very similar size distribution parameters for speaking normal, speaking loud and singing the selected song, irrespective of subject's experience and voice type, e.g. soprano, mezzosoprano, alto, tenor, baritone or bass. We also find very similar number concentrations for speaking loud and singing the selected song ($189\,L^{-1}$ compared to $188\,L^{-1}$). Singing "Happy Birthday" led to slightly lower particle number concentration ($160\,L^{-1}$) and the lowest emission was found for speaking normal ($148\,L^{-1}$). However, for all these activities the number concentrations are within a factor of 1.3 between the lowest and the highest, so we cannot rule out that the differences are explainable by between-subject variability.

The aggregated OPS data from subjects of the same age-category (within 5 years) shown in Fig. 14, suggests that there is also no significant difference in the particle size distribution between non-professional and semi-professional/professional singers, neither for speaking loud nor for singing "Happy Birthday". This is confirmed by a two-sided t-test on $N_{<5}$ for both groups. p values were 0.74 for speaking loud and 0.28 for singing "Happy Birthday". Even though the particle concentration emitted while singing a selected song is higher compared to singing "Happy Birthday" for the professional singers, this difference is still not statistically significant ($p = 0.11$).

4. Comparisons with data from the literature

In the previous sections, we have pointed out some similarities and differences with data from the literature. We also pointed out the shortcomings of that data and the gaps in knowledge that this study fills. Considering this, a detailed comparison with the prior literature is not trivial because the experimental conditions, the number of subjects involved, and the activities are highly variable in the various studies. For a true comparison, specific adjustments must be made to the prior data, which requires extensive justification and is therefore beyond the scope of this study (see, e.g., the discussions on the synthesis of such datasets in Pöhlker, et al. (2021)). However, we can point out two major differences that can be identified by a naive comparison of the (shape of) datasets shown in Fig. 6 with the prior published data.

The first major difference is, that the concentration of >1 μm particles during breathing is higher than most of those published previously (e.g. Almstrand, et al., 2010; Alsved, et al., 2020; Holmgren, et al., 2010; Morawska, et al., 2009a). This can be explained by the facts that our data are corrected for particle shrinkage by a factor of 4.5, while those used by others are smaller (typically by a factor of 2), publications present data not corrected for drying, or that the published data are modeled assuming hygroscopic behavior (see Section 2.9 for more detail). Some of the data published to date also suffer from a lack of environmental control during measurements, making corrections to the data ambiguous, if not impossible. As shown in Section 2.9, the shrinkage factor of 4.5 used in this study is justified since it was validated by independent experiments with human saliva and human airway surface fluid.

The second major difference to prior data is the location of particle concentration peak observed at >10 μm for vocalizations. While our data shows a peak in concentration at 30 μm–40 μm for these activities, the peak for previously published data is mostly around 100 μm though there is a very large scatter in the existing data Pöhlker, et al. (2021). Notable exceptions are the Duguid (indirect sizing, 1946) and Chao, et al. (direct sizing, 2009) measurements who found a peak around 10 μm and 16 μm-24 μm,

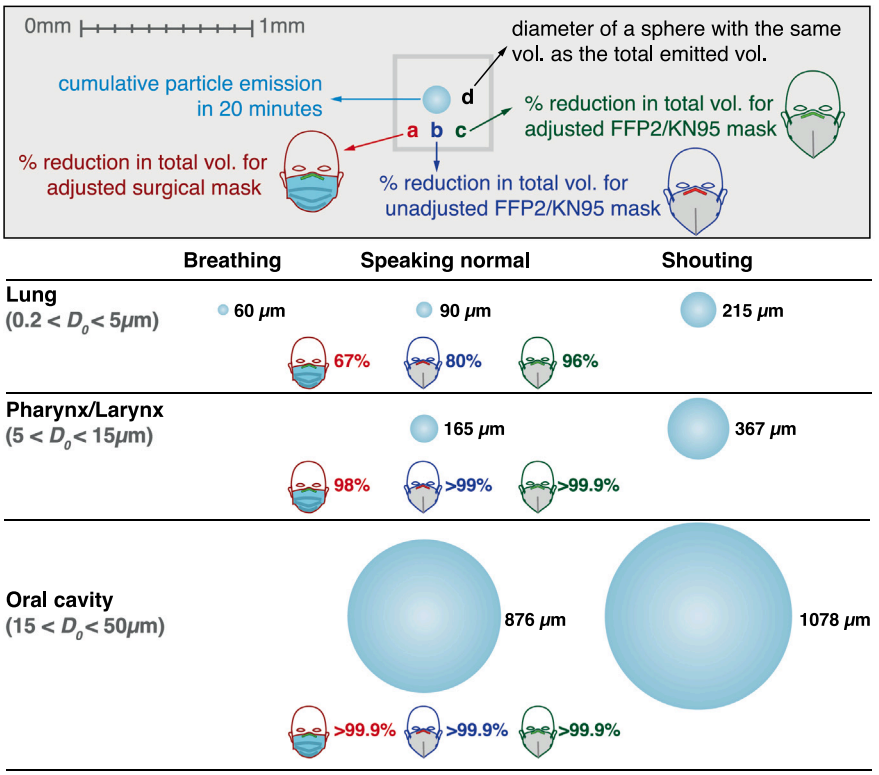

Fig. 15. Accumulated total particle volume emission during 20 min for different activities originating from different parts of the respiratory tract. The lognormal fits presented in Table 3 are used to produce results shown in this plot. A hard cutoff of 5 μm and 50 μm is considered for breathing and vocalization activity, respectively. For all three activities, a constant exhalation rate of $0.57\,m^3\,h^{-1}$ is assumed, which is close to the exhalation rate of an adult during breathing. Therefore, the total volume emissions shown for speaking and shouting are lower bounds for adults. The size-dependent total inward leakage for different masks and the fits used to calculate the influence of the mask were obtained from the median values of the measurements in Bagheri, et al. (2021). (For interpretation of the references to color in this figure legend, the reader is referred to the web version of this article.)

respectively. This discrepancy (or at least part of it) is due to the fact that in most previous studies particle size was measured indirectly (with a few exceptions, see Merghani, et al. (2021), Pöhlker, et al. (2021), and references therein). In these studies, the samples are usually deposited on a substrate, and the particle size before deposition had to be estimated from the impact size, taking into account different assumptions regarding evaporation and dispersion factor. In our study, we used in-line holography to measure geometric particle size directly in the air and only a few centimeters from the subjects' faces. Holography is a well-established tool in the field of cloud microphysics, and the instrument used here is regularly benchmarked against other measurement tools. It has also been re-calibrated for the measurements presented here, as explained previously.

5. Significance

Our data fill a major gap in our knowledge and help to better understand the airborne-transmission pathways of infectious agents. In addition, the data provide a range of information on how to propose and evaluate different intervention strategies in both the professional medical setting and the so-called public sector. Thus, they are a prerequisite for a more appropriate assessment of infection risk or prevention strategies. The number size distributions provided for respiratory particles in different activities allow for a robust and reliable calculation of infection risk in different environments and scenarios. As an example, it enables taking into account particle size for filtration through face masks and absorption in the respiratory tract of susceptible individuals to draw concrete control measures for policy makers, as shown in Bagheri, Thiede, Hejazi, Schlenczek, and Bodenschatz (2021).

In addition, knowledge of the site of origin and age dependence allows disease-specific calculation of infection risk and development of control strategies. For example, Fig. 15 shows the cumulative volume of exhaled particles during 20 min of breathing, speaking normally and shouting for the population mean. The emission of pathogens and the associated risk of infection transmission are directly related to the volume of emitted particles. The proportionality factor is the pathogen load, usually expressed by the number of pathogens per mL of respiratory fluid (from which the respiratory particles are generated). It has also been speculated that the pathogen load in the main fluid may be much lower than that of the generated particles (e.g. see Lai, et al., 2022 and references therein). Nevertheless, the direct correlation between the emitted volume and emitted pathogen remains.

From Fig. 15, it can be seen that the total volume emission originating from the lungs during 20 min of breathing is about a third of speaking normal ($= 60^3/90^3$) and about 2% of that produced during shouting ($= 60^3/215^3$). Compared to the particles produced in the URT, the PM5s are the most difficult to filter with face masks, as shown by the colored numbers for different masks/fits in Fig. 15. These results show that wearing face masks with high filtration efficiency and suitable cut for a tight fit, such as FFP2/KN95 masks, is associated with a protection factor — the ratio between the penetrated/leaked pathogen copies through the mask and the total emitted pathogen copies — of 96% for breathing, which increases to > 99.9% for vocalization activities.

To assess the risk of infection transmission as a function of pathogen features, activity and age, we should consider three disease-specific cases: (1) the pathogen load is only in the LRT, (2) the pathogen load is in both the LRT and the Upper Respiratory Tract (URT), and (3) the pathogen load is only in the URT.

In all cases, vocalization is associated with significantly higher cumulative particle volume, but especially in cases (2) and (3). In case (3), all masks considered here have similar effects on the pathogens emitted by the URT, while age is unlikely to be a significant factor.

The role of age and individual characteristics (i.e. low-/super-emitters) become important when the pathogen load is high in the lungs, i.e. cases (1) and (2). In general, the cumulative emitted volume of particles originating in the lungs, i.e. PM5, is much lower than in other areas of the respiratory tract, but it can become significant depending on the activity, age and individual characteristics. Age not only reduces PM5 volume concentration by a factor of 3 to 4 in children and adolescents during vocalization, but also the exhalation flow rate is reduced by a factor of ~ 2 in these age groups. This results in a maximum $\sim 6-8$-fold reduction in the cumulative emitted volume of PM5 compared with adults during vocalization. This is nearly the same effect as wearing a non-fitted FFP2 mask. Because PM5 produced during breathing is not age-dependent (see Section 3.2), the volume emitted by young individuals during breathing is about a factor of 2 lower than that emitted by adults, which is due only to the lower exhalation flow rate. Assuming that disease parameters are age-independent, younger individuals are less likely to infect others, especially in case (1).

With the regard to individual characteristics, we found that children and adolescents are less likely to trigger a super-spreading event if the disease characteristics fall into the category of case (1). In our database, there are some young individuals who emit $\sim 1\%$ of cumulative volume of PM5 compared to the population mean. The cumulative emitted volume of PM5 by these individuals is lower than an average adult wearing a well-fitting FFP2 mask. In contrast, the lowest PM5 emissions within the adult population result in about 10%–40% less PM5 volume compared to the population mean. Children and adolescent super-emitters produce at most 1.8 times the cumulative volume of PM5 emitted by the population mean, which would bring them close to the population mean taking into account their lower exhalation flow rates. In contrast, some adult super-emitters can emit cumulative volume of PM5 that is 11 times higher than the population average during breathing and about 5 times higher for vocalizations. These results suggest that for diseases that tend to have high pathogen loads in the LRT, cases (1) and (2), adults are particularly infectious when all other parameters remain unchanged.

Overall, our results show that for case (1), the use of masks with low total inward/outward leakage, such as FFP2, is particularly important for adults, whereas for children and adolescents, the use of surgical masks has a comparable impact on outward protection as FFP2 masks for adults. The use of surgical or fabric masks may be effective if the pathogen load is high in the URT alone, i.e., case (3). However, even in this case, there should be good reasons not to use masks with lower inward/outward leakage given the significant difference in performance. For case (2), in particular, the use of well-fitting FFP2 masks is the most effective control measure.

6. Conclusions

We presented data from 132 healthy subjects, aged 5 to 80 years, individually measured across the entire particle size range using a combination of in-line holography and particle spectrometry. Measurements are carried out under extremely well-controlled conditions and during everyday activities such as breathing, speaking and singing. We discussed the sites of origin of exhaled particles and the influence of biological age, BMI, gender, smoking and exercise habits, vocal sound pressure/pitch, subject variability, and breathing pattern/frequency on the size and concentration of exhaled particles from total and/or selected subsets of the measured data in detail. The main findings are as follow:

- a comprehensive dataset of the size and absolute concentration of particles in the nanometer to millimeter range exhaled during breathing and vocalization is provided with detailed statistics on global and per age-group low- and super-emitters,
- breathing produces mainly PM5 (i.e. particles with wet diameter $D_0 < 5$ μm), while vocalization can produce particles of up to several hundred micrometers,
- the highest particle number concentration produced by all the activities studied is found within the 0.1–1.0 μm diameter range,
- the secondary number-concentration peak observed in most vocalization activities is around 40 μm,
- the highest PM5 concentrations are produced by shouting, followed by singing, speaking loudly, speaking normally, and breathing,
- age is the most important parameter affecting PM5 concentration, resulting in a doubling of concentration over a 7-year period for adolescents and a 30-year period for adults,
- gender, body mass index, smoking or exercise habits have no discernible effect on PM5 concentration,
- particles with a diameter of <5 μm predominantly originate from the lower respiratory tract, 5-15 μm from the larynx/pharynx, and >15 μm from the oral cavity,

- PM5 concentration can vary by one order of magnitude within a person, while inter-person variability can span two orders of magnitude, largely explainable by difference in age,
- no discernible inter-person variability for particles larger than 5 μm is found,
- sound pressure/pitch was found to have an impact on PM5 particles, but the impact could be largely explained by the change in lung volume used,
- the multimodal lognormal fits provided (Table 4), which provide absolute concentrations over the entire relevant size range, in conjunction with the functions to account for the effect of age on PM5 (Fig. 7) and the knowledge of the particle origin in the respiratory tract, allow a detailed investigation of the risk of infection transmission and the routes of transmission as a function of pathogen characteristics, age, and activity,
- vocalizations have been found to be associated with higher cumulative-particle-volume emission and thus higher risk of infection transmission. The differences between breathing and vocalization become much more significant when the pathogen load in the upper respiratory tract is higher than that in the lower respiratory tract,
- for a given activity and duration, the cumulative emitted volume of PM5 by children is on average 6–8 times lower than that of an average adult,
- adults are more likely to spread airborne-transmitted respiratory diseases associated with a high pathogen load in the lower respiratory tract. They are also much more likely to trigger super-spreading events in such scenarios.

CRediT authorship contribution statement

Gholamhossein Bagheri: Designed the experimental procedures for the subject measurements, Conducted the experiments on the human subjects, Analysed and interpreted the data, Prepared the holography data, Wrote the draft of the main text, Writing the final text. **Oliver Schlenczek:** Designed the experimental procedures for the subject measurements, Conducted the experiments on the human subjects, Analysed and interpreted the data, Prepared the holography data, Wrote the draft of the main text, Writing the final text. **Laura Turco:** Designed the experimental procedures for the subject measurements, Conducted the experiments on the human subjects, Writing the final text. **Birte Thiede:** Designed the experimental procedures for the subject measurements, Conducted the experiments on the human subjects, Analysed and interpreted the data, Wrote the draft of the main text, Writing the final text. **Katja Stieger:** Conducted the experiments on the human subjects, Writing the final text. **Jana M. Kosub:** Conducted the experiments on the human subjects, Writing the final text. **Sigrid Clauberg:** Consulted on the interpretation of the data, Writing the final text. **Mira L. Pöhlker:** Consulted on the experiments, Consulted on the interpretation of the data, Writing the final text. **Christopher Pöhlker:** Consulted on the experiments, Consulted on the interpretation of the data, Writing the final text. **Jan Moláček:** Designed and conducted the ASL and saliva measurements, Writing the final text. **Simone Scheithauer:** Designed the experimental procedures for the subject measurements, Advised all medical aspects of the investigation, Consulted on the interpretation of the data, Writing the final text. **Eberhard Bodenschatz:** Designed the experimental procedures for the subject measurements, Wrote the ethics application, Conducted the experiments on the human subjects, Analysed and interpreted the data, Wrote the draft of the main text, Writing the final text.

Declaration of competing interest

The authors declare that they have no known competing financial interests or personal relationships that could have appeared to influence the work reported in this paper.

Data availability

The datasets generated and/or analyzed during the current study are available from the corresponding authors on reasonable request. A concise version of the dataset is freely available in the HEADS (Human Emission of Aerosol and 1290 Droplet Statistics) web-app at https://aerosol.ds.mpg.de/en/.

Acknowledgments

The authors would like to thank Udo Schminke and the machine shop of the Max Planck Institute for Dynamics and Self-Organisation (MPIDS) for their technical support during the campaign. We would also like to thank Freja Nordsiek from the MPIDS for fruitful discussions and analyzing the detection efficiency of the holographic setup, Katja Walter from the University Medical Center Göttingen (UMG) for assisting with the measurements on human subjects, Sarah Romanowski from the MPIDS for maintaining the cleanroom and providing the cleanroom equipment, Katharina Gunkel and Andreas Renner from the MPIDS for maintaining and disinfecting the isolation shields, Artur Kubitzek from the MPIDS for technical support and maintaining equipment, Jan-David Förster from the Max Planck Institute for Chemistry for participating in the campaign in February and Andreas Beste from the UMG for providing the ASL samples. We would like to thank our volunteers who came from the MPIDS, the UMG, the Hannover State Opera, the Hannover University of Music Theatre and Media, the Jacobi Kantorei Göttingen, the Brass Band Association of North Rhine-Westphalia, the Musikverein Oesdorf e.V., the Landeskoordinator Klassenmusizieren, the Evangelischer Posaunendienst and the local schools in Göttingen and Bad Sachsa. We would also like to thank the Max Planck Society for making research in this field possible.

Funding

This work has been partly funded by the BMBF (Federal Ministry of Education and Research), Germany as part of the B-FAST (Bundesweites Forschungsnetz Angewandte Surveillance und Testung) project (01KX2021) within the NUM (Netzwerk Universitätsmedizin), Deutsche Forschungsgemeinschaft, Germany (project number: 469107130) and the Max Planck Society, Germany. The funders had no role in study design, data collection and analysis, decision to publish, or preparation of the manuscript.

Ethics statement

The non-invasive exhaled particle sampling study which led to this paper was approved by the Ethics Commission of the Max Planck Society (Submission 2020_23). All subjects gave their written consent to data storage and analysis.

Appendix A. Supplementary data

Supplementary material related to this article can be found online at https://doi.org/10.1016/j.jaerosci.2022.106102.

References

Abkarian, M., & Stone, H. A. (2020). Stretching and break-up of saliva filaments during speech: A route for pathogen aerosolization and its potential mitigation. *Physical Review Fluids*, *5*, http://dx.doi.org/10.1103/PhysRevFluids.5.102301.

Almstrand, A.-C., Bake, B., Ljungström, E., Larsson, P., Bredberg, A., Mirgorodskaya, E., et al. (2010). Effect of airway opening on production of exhaled particles. *Journal of Applied Physiology*, *108*(3), 584–588.

Almstrand, A.-C., Ljungström, E., Lausmaa, J., Bake, B., Sjövall, P., & Olin, A.-C. (2009). Airway monitoring by collection and mass spectrometric analysis of exhaled particles. *Analytical Chemistry*, *81*(2), 662–668. http://dx.doi.org/10.1021/ac802055k.

Alsved, M., Matamis, A., Bohlin, R., Richter, M., Bengtsson, P.-E., Fraenkel, C.-J., et al. (2020). Exhaled respiratory particles during singing and talking. *Aerosol Science and Technology*, *54*, 1245–1248. http://dx.doi.org/10.1080/02786826.2020.1812502, URL: https://www.tandfonline.com/doi/full/10.1080/02786826.2020.1812502.

Anderson, W. H., Coakley, R. D., Button, B., Henderson, A. G., Zeman, K. L., Alexis, N. E., et al. (2015). The relationship of mucus concentration (hydration) to mucus osmotic pressure and transport in chronic bronchitis. *American Journal of Respiratory and Critical Care Medicine*, *192*(2), 182–190.

Asadi, S., Wexler, A. S., Cappa, C. D., Barreda, S., Bouvier, N. M., & Ristenpart, W. D. (2019). Aerosol emission and superemission during human speech increase with voice loudness. *Scientific Reports*, *9*, 2348. http://dx.doi.org/10.1038/s41598-019-38808-z, URL: http://www.nature.com/articles/s41598-019-38808-z.

Bagheri, G., Thiede, B., Hejazi, B., Schlenczek, O., & Bodenschatz, E. (2021). An upper bound on one-to-one exposure to infectious human respiratory particles. *Proceedings of the National Academy of Sciences*, *118*(49), Article e2110117118. http://dx.doi.org/10.1073/pnas.2110117118.

Bake, B., Larsson, P., Ljungkvist, G., Ljungström, E., & Olin, A.-C. (2019). Exhaled particles and small airways. *Respiratory Research*, *20*, 8. http://dx.doi.org/10.1186/s12931-019-0970-9, URL: https://respiratory-research.biomedcentral.com/articles/10.1186/s12931-019-0970-9.

Bechtold, B. (2016). Violin plots for matlab, github project. http://dx.doi.org/10.5281/zenodo.4559847. https://github.com/bastibe/Violinplot-Matlab.

Chao, C., Wan, M., Morawska, L., Johnson, G., Ristovski, Z., Hargreaves, M., et al. (2009). Characterization of expiration air jets and droplet size distributions immediately at the mouth opening. *Journal of Aerosol Science*, *40*, 122–133. http://dx.doi.org/10.1016/j.jaerosci.2008.10.003, URL: https://linkinghub.elsevier.com/retrieve/pii/S0021850208001882.

Duguid, J. (1946). The size and the duration of air-carriage of respiratory droplets and droplet-nuclei. *Epidemiology and Infection*, *44*, 471–479.

Effros, R. M., Hoagland, K. W., Bosbous, M., Castillo, D., Foss, B., Dunning, M., et al. (2002). Dilution of respiratory solutes in exhaled condensates. *American Journal of Respiratory and Critical Care Medicine*, *165*(5), 663–669.

Fabian, P., Brain, J., Houseman, E. A., Gern, J., & Milton, D. K. (2011). Origin of exhaled breath particles from healthy and human rhinovirus-infected subjects. *Journal of Aerosol Medicine and Pulmonary Drug Delivery*, *24*(3), 137–147. http://dx.doi.org/10.1089/jamp.2010.0815.

Fabian, P., McDevitt, J. J., DeHaan, W. H., Fung, R. O. P., Cowling, B. J., Chan, K. H., et al. (2008). Influenza virus in human exhaled breath: An observational study. *PLoS One*, *3*(7), Article e2691. http://dx.doi.org/10.1371/journal.pone.0002691.

Fugal, J. P., Schulz, T. J., & Shaw, R. A. (2009). Practical methods for automated reconstruction and characterization of particles in digital in-line holograms. *Measurement Science & Technology*, *20*(7), Article 075501.

Gregson, F. K. A., Watson, N. A., Orton, C. M., Haddrell, A. E., McCarthy, L. P., Finnie, T. J. R., et al. (2021). Comparing aerosol concentrations and particle size distributions generated by singing, speaking and breathing. *Aerosol Science and Technology*, 1–15. http://dx.doi.org/10.1080/02786826.2021.1883544.

Groth, R., Cravigan, L. T., Niazi, S., Ristovski, Z., & Johnson, G. R. (2021). In situ measurements of human cough aerosol hygroscopicity. *Journal of the Royal Society Interface*, *18*(178), Article 20210209.

Han, Z. Y., Weng, W. G., & Huang, Q. Y. (2013). Characterizations of particle size distribution of the droplets exhaled by sneeze. *Journal of the Royal Society Interface*, *10*(88), Article 20130560. http://dx.doi.org/10.1098/rsif.2013.0560.

Haslbeck, K., Schwarz, K., Hohlfeld, J. M., Seume, J. R., & Koch, W. (2010). Submicron droplet formation in the human lung. *Journal of Aerosol Science*, *41*(5), 429–438. http://dx.doi.org/10.1016/j.jaerosci.2010.02.010, URL: http://www.sciencedirect.com/science/article/pii/S0021850210000431.

Hill, D. B., Vasquez, P. A., Mellnik, J., McKinley, S. A., Vose, A., Mu, F., et al. (2014). A biophysical basis for mucus solids concentration as a candidate biomarker for airways disease. *PLoS One*, *9*(2), Article e87681.

Holmgren, H., Bake, B., Olin, A.-C., & Ljungström, E. (2011). Relation between humidity and size of exhaled particles. *Journal of Aerosol Medicine and Pulmonary Drug Delivery*, *24*, 253–260. http://dx.doi.org/10.1089/jamp.2011.0880, URL: http://www.liebertpub.com/doi/10.1089/jamp.2011.0880.

Holmgren, H., Gerth, E., Ljungstrom, E., Larsson, P., Almstrand, A. C., Bake, B., et al. (2013). Effects of breath holding at low and high lung volumes on amount of exhaled particles. *Respiratory Physiology & Neurobiology*, *185*(2), 228–234. http://dx.doi.org/10.1016/j.resp.2012.10.010.

Holmgren, H., Ljungström, E., Almstrand, A.-C., Bake, B., & Olin, A.-C. (2010). Size distribution of exhaled particles in the range from 0.01 to 2.0μm. *Journal of Aerosol Science*, *41*(5), 439–446. http://dx.doi.org/10.1016/j.jaerosci.2010.02.011, URL: http://www.sciencedirect.com/science/article/pii/S0021850210000443.

Johnson, G. R., & Morawska, L. (2009). The mechanism of breath aerosol formation. *Journal of Aerosol Medicine and Pulmonary Drug Delivery*, *22*, 229–237. http://dx.doi.org/10.1089/jamp.2008.0720, URL: http://www.liebertpub.com/doi/10.1089/jamp.2008.0720.

Johnson, G., Morawska, L., Ristovski, Z., Hargreaves, M., Mengersen, K., Chao, C., et al. (2011). Modality of human expired aerosol size distributions. *Journal of Aerosol Science*, *42*, 839–851. http://dx.doi.org/10.1016/j.jaerosci.2011.07.009, URL: https://linkinghub.elsevier.com/retrieve/pii/S0021850211001200.

Lai, K.-M., Bottomley, C., & McNerney, R. (2011). Propagation of respiratory aerosols by the Vuvuzela. *PLoS One*, *6*(5), Article e20086. http://dx.doi.org/10.1371/journal.pone.0020086.

Lai, J., Coleman, K. K., Sheldon Tai, S.-H., German, J., Hong, F., Albert, B., et al. (2022). *Evolution of SARS-CoV-2 shedding in exhaled breath aerosols*. Cold Spring Harbor Laboratory Press, http://dx.doi.org/10.1101/2022.07.27.22278121, MedRxiv. arXiv:https://www.medrxiv.org/content/early/2022/08/01/2022.07.27.22278121.full.pdf, URL: https://www.medrxiv.org/content/early/2022/08/01/2022.07.27.22278121.

Lee, J., Yoo, D., Ryu, S., Ham, S., Lee, K., Yeo, M., et al. (2019). Quantity, size distribution, and characteristics of cough-generated aerosol produced by patients with an upper respiratory tract infection. *Aerosol and Air Quality Research*, *19*(4), 840–853. http://dx.doi.org/10.4209/aaqr.2018.01.0031, URL: http://dx.doi.org/10.4209/aaqr.2018.01.0031.

Li, L., Niu, M., & Zhu, Y. (2020). Assessing the effectiveness of using various face coverings to mitigate the transport of airborne particles produced by coughing indoors. *Aerosol Science and Technology*, 1–12. http://dx.doi.org/10.1080/02786826.2020.1846679.

Lieber, C., Melekidis, S., Koch, R., & Bauer, H.-J. (2021). Insights into the evaporation characteristics of saliva droplets and aerosols: Levitation experiments and numerical modeling. *Journal of Aerosol Science*, *154*, Article 105760. http://dx.doi.org/10.1016/j.jaerosci.2021.105760.

Loudon, R. G., & Roberts, R. M. (1967). Droplet expulsion from the respiratory tract. *American Review of Respiratory Disease*, *95*(3), 435–442.

Merghani, K. M. M., Sagot, B., Gehin, E., Da, G., & Motzkus, C. (2021). A review on the applied techniques of exhaled airflow and droplets characterization. *Indoor Air*, *31*, 7–25. http://dx.doi.org/10.1111/ina.12770, URL: https://onlinelibrary.wiley.com/doi/10.1111/ina.12770.

Morawska, L., Johnson, G., Ristovski, Z., Hargreaves, M., Mengersen, K., Chao, C., et al. (2008). Droplets expelled during human expiratory activities and their origin. In B. W. Olesen, J. Toftum, P. Wargocki, D. Zukowska, P. Strom-Tejsen (Eds.), *Proceeding of the 11th international conference on indoor air quality and climate change* (pp. 1–8). Denmark: University of Denmark, URL: https://eprints.qut.edu.au/15416/.

Morawska, L., Johnson, G. R., Ristovski, Z. D., Hargreaves, M., Mengersen, K., Corbett, S., et al. (2009a). Size distribution and sites of origin of droplets expelled from the human respiratory tract during expiratory activities. *Journal of Aerosol Science*, *40*, 256–269. http://dx.doi.org/10.1016/j.jaerosci.2008.11.002.

Morawska, L., Johnson, G. R., Ristovski, Z. D., Hargreaves, M., Mengersen, K., Corbett, S., et al. (2009b). Size distribution and sites of origin of droplets expelled from the human respiratory tract during expiratory activities. *Journal of Aerosol Science*, *40*(3), 256–269. http://dx.doi.org/10.1016/j.jaerosci.2008.11.002, URL: http://www.sciencedirect.com/science/article/pii/S0021850208002036.

Mürbe, D., Kriegel, M., Lange, J., Schumann, L., Hartmann, A., & Fleischer, M. (2021). Aerosol emission of adolescents voices during speaking, singing and shouting. *PLoS One*, *16*(2), Article e0246819. http://dx.doi.org/10.1371/journal.pone.0246819.

Nicas, M., Nazaroff, W. W., & Hubbard, A. (2005). Toward Understanding the Risk of Secondary Airborne Infection: Emission of Respirable Pathogens. *Journal of Occupational and Environmental Hygiene*, *2*, 143–154. http://dx.doi.org/10.1080/15459620590918466.

Papineni, R. S., & Rosenthal, F. S. (1997). The size distribution of droplets in the exhaled breath of healthy human subjects. *Journal of Aerosol Medicine*, *10*(2), 105–116. http://dx.doi.org/10.1089/jam.1997.10.105.

Pöhlker, M. L., Krüger, O. O., Förster, J.-D., Berkemeier, T., Elbert, W., Fröhlich-Nowoisky, J., et al. (2021). Respiratory aerosols and droplets in the transmission of infectious diseases. arXiv pre-print, 2103.01188.

Randall, K., Ewing, E. T., Marr, L., Jimenez, J., & Bourouiba, L. (2021). How did we get here: What are droplets and aerosols and how far do they go? A historical perspective on the transmission of respiratory infectious diseases. SSRN.

Romanò, F., Muradoglu, M., Fujioka, H., & Grotberg, J. (2021). The effect of viscoelasticity in an airway closure model. *Journal of Fluid Mechanics*, *913*, A31. http://dx.doi.org/10.1017/jfm.2020.1162.

Schlenczek, O. (2018). *Airborne and ground-based holographic measurement of hydrometeors in liquid-phase, mixed-phase and ice clouds* (Ph.D. thesis), (p. 304). University of Mainz.

Schwarz, K., Biller, H., Windt, H., Koch, W., & Hohlfeld, J. M. (2010). Characterization of exhaled particles from the healthy human lung—A systematic analysis in relation to pulmonary function variables. *Journal of Aerosol Medicine and Pulmonary Drug Delivery*, *23*(6), 371–379. http://dx.doi.org/10.1089/jamp.2009.0809.

Schwarz, K., Biller, H., Windt, H., Koch, W., & Hohlfeld, J. M. (2015). Characterization of exhaled particles from the human lungs in airway obstruction. *Journal of Aerosol Medicine and Pulmonary Drug Delivery*, *28*(1), 52–58. http://dx.doi.org/10.1089/jamp.2013.1104.

Siegel, J. D., Rhinehart, E., Jackson, M., & Chiarello, L. (2007). 2007 Guideline for isolation precautions: preventing transmission of infectious agents in health care settings. *American Journal of Infection Control*, *35*(10), S65–S164.

Smith, S. H., Somsen, G. A., Van Rijn, C., Kooij, S., Van Der Hoek, L., Bem, R. A., et al. (2020). Aerosol persistence in relation to possible transmission of SARS-CoV-2. *Physics of Fluids*, *32*(10), Article 107108.

Song, D., Cahn, D., & Duncan, G. A. (2020). Mucin biopolymers and their barrier function at airway surfaces. *Langmuir*, *36*(43), 12773–12783.

Stiti, M., Castanet, G., Corber, A., Alden, M., & Berrocal, E. (2022). Transition from saliva droplets to solid aerosols in the context of COVID-19 spreading. *Environmental Research*, *204*, Article 112072.

von der Weiden, S.-L., Drewnick, F., & Borrmann, S. (2009). Particle loss calculator – a new software tool for the assessment of the performance of aerosol inlet systems. *Atmospheric Measurement Techniques*, *2*(2), 479–494. http://dx.doi.org/10.5194/amt-2-479-2009, URL: https://amt.copernicus.org/articles/2/479/2009/.

Xie, X., Li, Y., Sun, H., & Liu, L. (2009). Exhaled droplets due to talking and coughing. *Journal of the Royal Society Interface*, *6*(suppl_6), S703–S714.